Check for updates

Deletion of *Yersinia pestis ail* Causes Temperature-Sensitive Pleiotropic Effects, Including Cell Lysis, That Are Suppressed by Carbon Source, Cations, or Loss of Phospholipase A Activity

Anna M. Kolodziejek,[b] Carolyn J. Hovde,[a] Gregory A. Bohach,[b]* Scott A. Minnich[a]

[a]Department of Animal, Veterinary, and Food Science, University of Idaho, Moscow, Idaho, USA
[b]Department of Microbiology, Molecular Biology, and Biochemistry, University of Idaho, Moscow, Idaho, USA

Carolyn J. Hovde and Scott A. Minnich contributed equally to this work.

ABSTRACT Maintenance of phospholipid (PL) and lipopoly- or lipooligosaccharide (LPS or LOS) asymmetry in the outer membrane (OM) of Gram-negative bacteria is essential but poorly understood. The *Yersinia pestis* OM Ail protein was required to maintain lipid homeostasis and cell integrity at elevated temperature (37°C). Loss of this protein had pleiotropic effects. A *Y. pestis* Δ*ail* mutant and KIM6^{+} wild type were systematically compared for (i) growth requirements at 37°C, (ii) cell structure, (iii) antibiotic and detergent sensitivity, (iv) proteins released into supernatants, (v) induction of the heat shock response, and (vi) physiological and genetic suppressors that restored the wild-type phenotype. The Δ*ail* mutant grew normally at 28°C but lysed at 37°C when it entered stationary phase, as shown by cell count, SDS-PAGE of cell supernatants, and electron microscopy. Immunofluorescence microscopy showed that the Δ*ail* mutant did not assemble Caf1 capsule. Expression of heat shock promoter *rpoE* or *rpoH* fused to a *lux* operon reporter were not induced when the Δ*ail* mutant was shifted from 28°C to 37°C ($P < 0.001$ and $P < 0.01$, respectively). Mutant lysis was suppressed by addition of 11 mM glucose, 22 or 44 mM glycerol, 2.5 mM Ca^{2+}, or 2.5 mM Mg^{2+} to the growth medium or by a mutation in the phospholipase A gene (*pldA*::miniTn*5*, Δ*pldA*, or PldA[S164A]). A model accounting for the temperature-sensitive lysis of the Δ*ail* mutant and the Ail-dependent stabilization of the OM tetraacylated LOS at 37°C is presented.

IMPORTANCE The Gram-negative pathogen *Yersinia pestis* transitions between a flea vector (ambient temperature) and a mammalian host (37°C). In response to 37°C, *Y. pestis* modifies its outer membrane (OM) by reducing the fatty acid content in lipid A, changing the outer leaflet from being predominantly hexaacylated to being predominantly tetraacylated. It also increases the Ail concentration, so it becomes the most prominent OM protein. Both measures are needed for *Y. pestis* to evade the host innate immune response. Deletion of *ail* destabilizes the OM at 37°C, causing the cells to lyse. These results show that a protein is essential for maintaining lipid asymmetry and lipid homeostasis in the bacterial OM.

KEYWORDS *Yersinia pestis*, Ail, lysis, phospholipid, PldA, LPS, heat shock response, membrane homeostasis, thermosensitivity

Even with exquisite knowledge of the composition and architecture of cell membranes, it is not yet understood how lipid and protein interactions maintain the integrity and stability of this essential barrier. One model of membrane analysis has been the Gram-negative bacterial outer membrane (OM), which is the primary barrier against harsh external environments and is comprised of an asymmetric lipid bilayer embedded with numerous proteins (1). Under physiological conditions, the outer

leaflet of the Gram-negative OM contains lipopolysaccharide (LPS) or lipooligosaccharide (LOS). LPS consists of three components: (i) an anchoring lipid A moiety, which is a phosphorylated glucosamine dimer acylated with four to seven fatty acids depending on the Gram-negative species and environmental conditions, (ii) a highly conserved core sugar moiety, and (iii) a distal carbohydrate O-antigen, which can vary significantly even within strains of the same species. The inner leaflet of the OM and the cytoplasmic membrane contains glycerophospholipids (PL) (1). Under stress conditions (i.e., exposure to chelating agents or removal of OM proteins [OMPs]) or when LPS transport or synthesis genes are disrupted, PL from the inner leaflet are directed to the OM outer leaflet to compensate for reduced LPS concentration or disorganization. This results in PL patches within the OM outer leaflet (2, 3). When PL from the OM inner leaflet are insufficient to compensate for perturbations, the cell can traffic PL from the cytoplasmic membrane (4).

Because the presence of surface-exposed PL reduces OM barrier functions, the PL concentration must be controlled (3, 5). Phospholipase A (PldA) is an OM enzyme that catalyzes the hydrolysis of a wide range of PL substrates present in the OM outer leaflet by removal of the sn-1 and sn-2 fatty acid side chains from the glycerophosphodiester backbone of both PL and lysophospholipid (lyso-PL) (6). PldA resides in the OM as an inactive monomer under normal conditions. However, when membrane perturbations occur and PL or lyso-PL are present in the OM outer leaflet, PldA forms an active dimer with the catalytic site located in the OM outer leaflet (6). Additionally, PagP, a palmitoyltransferase, removes palmitate from PL at the sn-1 position and transfers it to lipid A. A third component for balancing OM composition is the Mla (maintenance of lipid asymmetry) system best studied in *Escherichia coli*. This system is an ABC transporter that regulates transport of PL between the OM outer leaflet and the cytoplasmic membrane (4, 7–9).

Yersinia pestis is a uniquely beneficial model to investigate membrane integrity, because it adapted its OM composition by genomic reduction for survival in its flea vector and to be highly virulent in mammalian hosts. Adaptations due to gene loss include a set of mutations in the O-antigen gene cluster such that lipid A is only capped by core oligiosaccharides (10). Shortened LOS is required for the type III secretion (T3SS) organelle and Ail (attachment and invasin locus) protein access to eukaryotic host cells (11, 12). The plasmid-encoded T3SS is induced at 37°C and confers a poorly understood temperature dependence for 2.5 mM Ca^{2+}; loss of the pCD1 virulence plasmid or mutations in this plasmid-encoded T3SS negate this requirement for Ca^{2+}. Additionally, at 37°C the lipid A of *Y. pestis* is predominantly tetraacylated rather than predominantly hexaacylated, as it is at 28°C. This reduced acylation at mammalian temperature obscures this pathogen-associated pattern molecule from Toll-like receptor 4 (TLR-4), allowing evasion of the innate immune response. The latter characteristic is due to a deletion of *lpxL* and a point mutation in *pagP* (13). Restoration of either gene restores hexaacylation of lipid A at 37°C with concomitant activation of TLR-4. *Y. pestis* with a functional *lpxL* gene is completely attenuated for virulence (14). In summary, temperature has a profound effect on acylation so that, at 28°C, LOS is hexaacylated and at 37°C it is tetraacylated.

The Ail/OmpX/PagC/Lom protein family consists of virulence-related OMPs found in *E. coli* (OmpX, Lom) (15, 16), *Klebsiella pneumoniae* (OmpK17) (17), *Cronobacter sakazakii* (18), *Enterobacter cloacae* (OmpX) (19), *Salmonella enterica* serovar Typhimurium (PagC, Rck) (20), *Y. enterocolitica* (Ail) (21), *Y. pseudotuberculosis* (Ail) (22), and *Y. pestis* Ail protein (*y1324*), also known as OmpX. *Y. pestis* Ail is a required virulence factor (23). Ail confers resistance to mammalian sera (11, 12, 24, 25), promotes bacterial adhesion to and invasion of host cells (11, 24, 26), and facilitates delivery of T3SS effectors to epithelial cells and leukocytes (26, 27). It also inhibits the inflammatory response and polymorphonuclear leukocyte recruitment to the lymph nodes (26, 28). Distinct from its homologues in other pathogenic yersiniae, *Y. pestis* Ail is expressed at both ambient (28°C) and mammalian host (37°C) temperatures (12, 21, 24, 29). It is the major protein

component in the *Y. pestis* OM fraction, comprising an estimated 20 to 30% of the total OM proteome at 37°C, the optimal temperature for its expression (30).

Temperature regulation defines the successful life cycle of *Y. pestis*, as it replicates in the flea vector or mammalian host. This intricate mechanism of temperature sensing coupled to gene regulation assists the bacterium in adapting to these dramatically different conditions (31). Acquisition of a virulence-associated plasmid, pFra/pMT1, encoding murine toxin and the *caf* operon, was at the origin of *Y. pestis* divergence from enteropathogenic *Y. pseudotuberculosis* (32). The *caf* operon encodes fimbrial Caf1 protein and a chaperone-usher system allowing its export and assembly on the *Y. pestis* surface as a capsule (33). Together with the T3SS, the capsule suppresses phagocytosis (34, 35). Importantly, capsule assembly is temperature regulated, and the *caf1* gene is one of the most transcribed genes during mammalian infection (36).

Heat shock response is a signaling pathway responsible for temperature sensing and activation of cellular responses crucial for survival at elevated temperatures (37). Initially described to mitigate stress at elevated temperatures due to accumulation of misfolded and aggregated proteins, it was also shown to regulate other cellular components, such as PL and LPS (38, 39). In *E. coli*, two alternative sigma factors involved in heat shock response were described, *rpoH* and *rpoE*, responding to alterations in cytoplasm and bacterial envelope, respectively (37, 40).

Under steady-state growth conditions, RpoE is sequestered in the cell by an inner membrane-bound anti-sigma factor, RseA. Upon an increase in the rate of misfolded OM proteins in the periplasmic space, RpoE is released due to RseA cleavage by the activated DegS protease (41). Because the increase in the rate of protein misfolding is induced with increasing growth temperature (42), RpoE has a pivotal thermoregulatory role in extracytoplasmic and heat shock responses.

Subsequent to our previously reported Ail-dependent virulence phenotypes (11, 24), here we describe the unique role of Ail in maintaining lipid homeostasis in the OM at elevated temperature. A *Y. pestis* Δ*ail* mutant and KIM6$^+$ wild type were systematically compared for (i) growth requirements at 37°C, (ii) cell structure, (iii) antibiotic and detergent sensitivity, (iv) analysis of proteins released into supernatants, (v) induction of the heat shock response, and (vi) physiological and genetic suppressors that restored the wild-type phenotype.

This is the first description of a thermoregulatory component to OM stability that involved Ail. Genetic and imaging data also support a recently described model of PL flow between bilayers of the OM and cytoplasmic membrane in *E. coli* (4). The findings contribute to the broader understanding of the dynamics between proteins and PL required for membrane stability in Gram-negative bacteria.

RESULTS

***Y. pestis* Δ*ail* mutant released proteins and lysed in stationary phase at 37°C.** Broth cultures of *Y. pestis* KIM6$^+$ Δ*ail* mutant underwent a significant decrease in turbidity after they reached stationary phase when grown at 37°C (Fig. 1A). Culture supernatants from the stationary phase (24 h postinoculation) were collected, filtered sterilized to remove cells and particulate debris, and precipitated. Significantly more supernatant proteins were recovered from the Δ*ail* mutant grown at 37°C than with the wild-type parental strain or the Δ*ail*-complemented strain (Fig. 1B). No cells grown at 28°C, including the Δ*ail* mutant, released differential or significant amounts of protein into the supernatant (Fig. 1B). Plate counts showed a 10-fold decrease in viability for the Δ*ail* mutant (data not shown). Transmission electron microscopy (TEM) imaging further confirmed cell death, revealing cell lysis of Δ*ail* in the stationary phase (Fig. 1C). The Δ*ail* mutant phenotype had increased lysis and protein release at mammalian host (37°C) but not flea vector (28°C) temperatures.

To investigate if the Δ*ail* mutant lysis was specific to this protein, Ail (*y1324*) and three other Ail homologs in the *Y. pestis* genome (*y1682*, *y2446*, and *y2034*) were overexpressed in *trans* under an isopropyl-β-D-thiogalactopyranoside (IPTG)-inducible
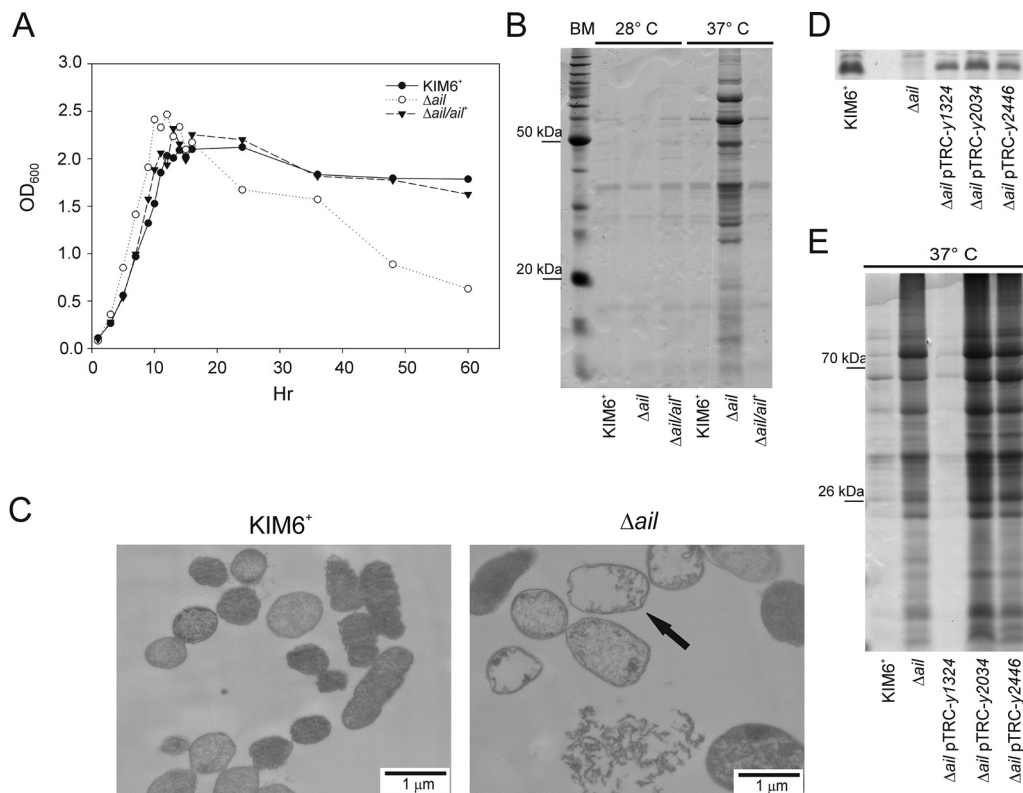
FIG 1 *Y. pestis* Δ*ail* mutant released proteins and lysed in stationary phase at 37°C. *Y. pestis* KIM6+ wild type, the Δ*ail* mutant, and the Δ*ail/ail*+ complemented strain were grown with aeration to late stationary phase at 37°C or 28°C in Luria-Bertani (LB) broth. (A) Growth measured by OD_{600} shows that only the Δ*ail* mutant grown at 37°C had a significant decrease in turbidity. (B) Cell-free supernatants from cultures grown for 24 h/37°C were ethanol precipitated, separated by 12.5% SDS-PAGE, and stained with Coomassie blue (bench mark standards [BM] on left). Only the Δ*ail* mutant grown at 37°C shows increased amounts of proteins released into the medium. (C) Representative transmission electron microscopy of 24 h/37°C cultures of KIM6+ and the Δ*ail* mutant are shown. The Δ*ail* mutant had increased cell ghosts (arrow) and released debris. (D) Ail or Ail homologues in *Y. pestis* KIM6+ wild type, the Δ*ail* mutant, and the Δ*ail* mutant complemented with *y1324* (control), *y2034*, or *y2446*; cells were grown to mid-exponential phase in medium with 1 mM IPTG. SDS-PAGE of whole-cell lysates stained with Coomassie blue, 15- to 20-kDa range shown. (E) Proteins released from cells as indicated in panel D. Cell-free supernatants were prepared as described for panel B, and BM standard positions are indicated on the left. Only KIM6+ and the Δ*ail* mutant expressing *y1324* did not release increased amounts of protein into the supernatant.

promoter in the Δ*ail* mutant as described previously by Bartra et al. (12) and tested for lysis. All constructs efficiently express the proteins in similar quantities (Fig. 1D) (12). Of the four proteins, only complementation with Ail (*y1324*) inhibited lysis of the Δ*ail* mutant (Fig. 1E). All cultures expressing Ail homologs lost turbidity after 72 h of growth, except for the Δ*ail* pTRC-*y1682* strain, which grew slowly and had reduced turbidity after 6 days (data not shown). Because of this difference in growth rate, the Δ*ail* pTRC-*y1682* strain was not included in the protein release assay (Fig. 1E). Interestingly, expression of *y2446* restored autoaggregation, a phenotype associated with Ail, but did not rescue cells from lysis (data not shown).

Together, these results showed that the deletion of *ail* affected *Y. pestis* cell stability and viability at 37°C. This effect was specific to the loss of Ail, as overexpression of the Ail homologs did not compensate for its loss.

Y. pestis Δ*ail* mutant grown at 37°C had membrane defects in stationary phase. To characterize changes in membrane properties between the Δ*ail* mutant and KIM6+ wild type, resistance to various membrane-active agents were compared (Table 1). Growth in the presence of antibiotic or detergent was not inhibited. Even though the Δ*ail* mutant was slightly more permeable to the cationic peptide polymyxin B, the MIC values for vancomycin and novobiocin indicated that the OM barrier of the Δ*ail* mutant

TABLE 1 Antibiotic and SDS susceptibility of *Y. pestis* KIM6$^+$ and the Δ*ail* mutant

Compound	MIC^a (μg/ml) or IC$_{50}$^{b} (μg/ml) for:	
	KIM6^{+c}	Δ*ail* mutant^c
Vancomycin	>4,000	>4,000
Novobiocin	50	100
Polymyxin B	1,000	250
SDS^d	226	329

^{a}MICs are for vancomycin, novobiocin, and polymyxin B.
^{b}IC$_{50}$, half-maximal inhibitory concentration, applies only to SDS.
^{c}*Y. pestis* grown in LB broth at 37°C for 24 h.
^{d}Sodium dodecyl sulphate.

was not changed. These properties were confirmed by a standard disc diffusion assay (data not shown). Further evidence that the OM of the Δ*ail* mutant remained functionally intact during growth was that it was slightly more resistant to the SDS anionic detergent than the KIM6$^+$ wild type (Table 1).

The observations described above were corroborated by TEM imaging of bacteria collected in the mid-exponential and stationary phases of growth. Cells during logarithmic-phase growth appeared to have intact OMs. Representative images of KIM6$^+$ wild type and the Δ*ail* mutant are shown in Fig. 2A. Nonetheless, there was release of
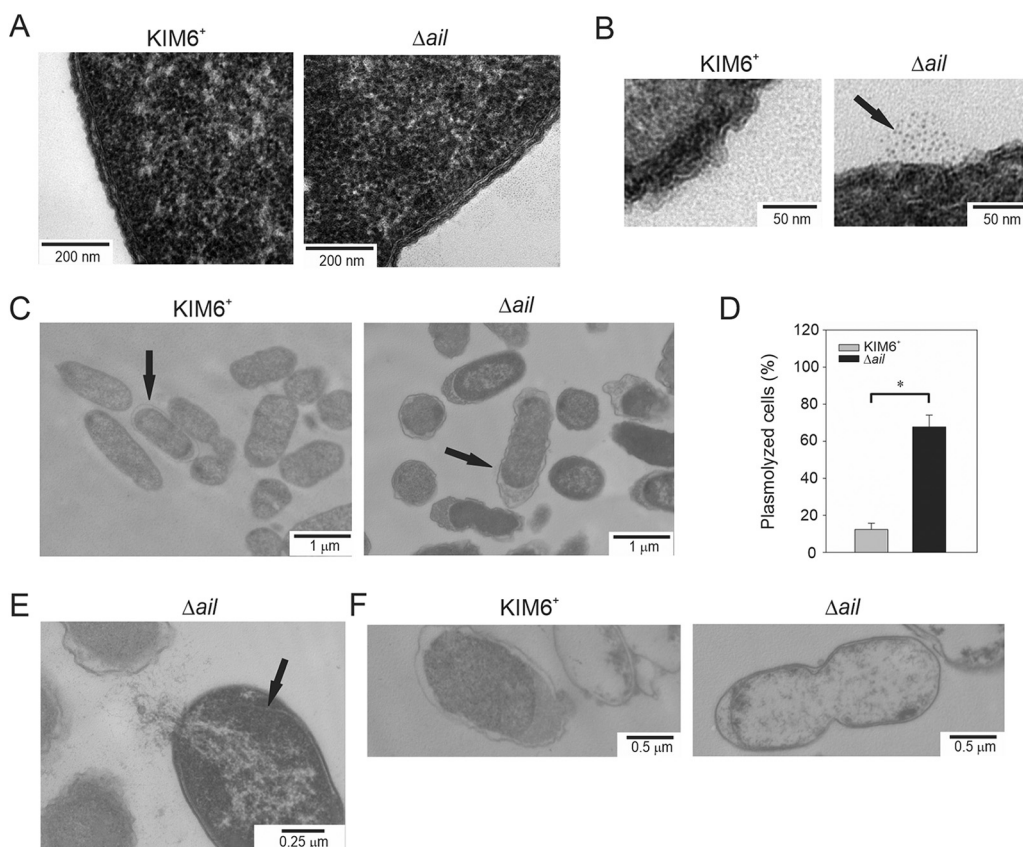

FIG 2 *Y. pestis* Δ*ail* mutant grown at 37°C had membrane defects in stationary phase. *Y. pestis* KIM6$^+$ wild type and the Δ*ail* mutant were grown with aeration at 37°C in Luria-Bertani (LB) broth. Representative transmission electron micrographs of cells in the logarithmic phase (OD$_{600}$ of 0.6) or 24 h at stationary phase are shown. In logarithmic phase, both cell types retained continuous membranes with no visible breaks or inner membrane retraction (A), but the Δ*ail* mutant released cellular matter into the supernatant (arrow) (B). In stationary phase, the Δ*ail* mutant had increased central cytoplasmic density, retracted inner membranes, enlarged periplasmic spaces (arrow) (C) and bursting cells with retracted inner membranes (arrow) (E). (F) In stationary phase, both KIM6$^+$ wild type and the Δ*ail* mutant had swollen ghost cells with decreased density. (D) Percent plasmolyzed cells was quantified from 21 electron micrographs; results are means ± standard errors (SE); an asterisk indicates statistical difference (Student's *t* test, $P < 0.05$).
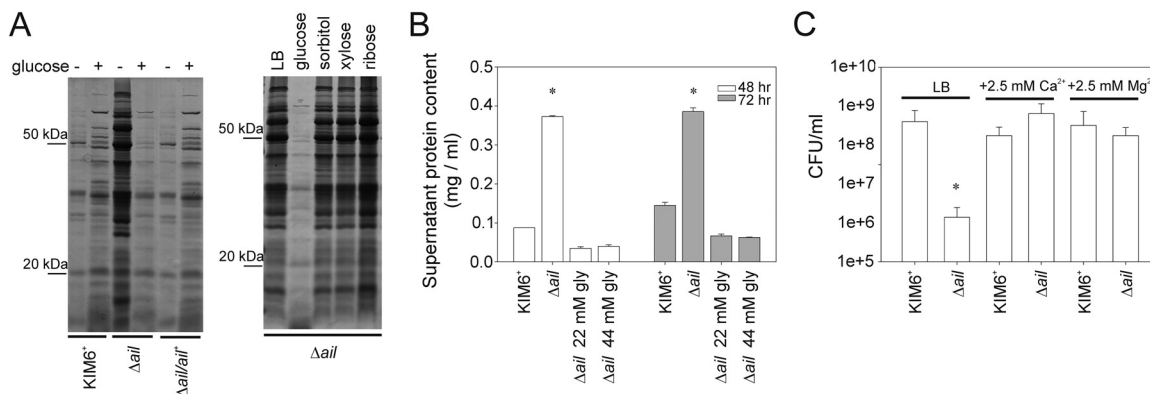
FIG 3 *Y. pestis* Δ*ail* mutant lysis at 37°C was prevented by glucose, glycerol, Ca^{2+}, or Mg^{2+}. *Y. pestis* KIM6$^+$ wild type, the Δ*ail* mutant, and the Δ*ail*/*ail*$^+$ complemented strain were grown with aeration to late stationary phase (48 h/37°C) in Luria-Bertani (LB) broth with or without carbohydrate or divalent cations. (A) Cell-free supernatants from cultures grown with or without 11 mM glucose, sorbitol, xylose, or ribose, as indicated, were ethanol precipitated, separated by 12.5% SDS-PAGE, and stained with Coomassie blue. Protein bench mark standard positions are indicated on the left. Only growth with glucose decreased the amounts of protein released into the medium by *Y. pestis* Δ*ail* mutant. (B) The protein content of cell-free supernatants from cultures grown with or without 22 mM or 44 mM glycerol was quantified by Bradford assays. Both glycerol concentrations decreased the amounts of protein released into the medium by *Y. pestis* Δ*ail* mutant. (C) After growth in LB with or without $CaCl_2$ or $MgCl_2$ (2.5 mM), numbers of CFU per milliliter were determined by plate count. Growth with either divalent cation prevented *Y. pestis* Δ*ail* mutant lysis. Protein quantification and number of CFU are means ± SE from two assays performed in duplicate on separate days; asterisks indicate statistical difference (ANOVA, $P < 0.05$).

small particles (approximately 3.5 nm in diameter) that was uniquely associated with all Δ*ail* mutant cells (Fig. 2B) and not observed with the KIM6$^+$ wild-type cells. Imaging of the cells collected during stationary phase showed more profound differences (Fig. 2C). Quantifying this difference, 67.7% of intact Δ*ail* mutant cells were undergoing plasmolysis (Fig. 2D). Cells had the characteristic detached inner membranes, enlarged periplasmic spaces, and condensation of intracellular matter. Only 12.3% of the wild-type KIM6$^+$ cells showed this characteristic. Among the Δ*ail* mutants, lysing cells were also observed, and a representative image is shown in Fig. 2E. Ghost cells, defined by two membranes with inner membrane detachment and loss of intracellular matter, were seen among both the Δ*ail* mutant and KIM6$^+$ wild type (Fig. 2F), with fewer ghost cells in the KIM6$^+$ wild-type images.

Together, results from membrane permeability assays and observations by TEM showed the membrane of the Δ*ail* mutant remained intact during exponential growth.

Y. pestis Δail mutant lysis was inhibited by selected carbon metabolites and divalent metal ions. Because the Δ*ail* mutant replicated efficiently and reached maximal growth similar to that of the KIM6$^+$ wild type and lysis was not observed until stationary phase, addition of carbon substrates or salts to the medium was tested. Glucose (11 mM) or glycerol (22 mM or 44 mM) inhibited lysis, as indicated by decreases in protein release to the supernatant (Fig. 3A and B). Even after prolonged incubation, the Δ*ail* mutant maintained turbidity similar to that of the KIM6$^+$ wild-type cultures (data not shown). Other carbon substrate additions either failed to inhibit lysis (11 mM sorbitol or 11 mM xylose) or slightly promoted lysis (11 mM ribose), demonstrating that inhibition of Δ*ail* lysis was specific to glucose and glycerol (Fig. 3A).

All pathogenic *Y. pestis* strains require 2.5 mM Ca^{2+} at 37°C due to the virulence plasmid pCD1, and loss of the plasmid negates this calcium dependence. Interestingly, the Δ*ail* mutant in the calcium-dependent KIM5 (pCD1$^+$) background did not lyse (data not shown). Because of this observation, even though KIM6$^+$ (pCD1$^-$) does not require Ca^{2+}, the addition of cations was tested. In KIM6$^+$, the Δ*ail* mutant grew similarly to KIM6$^+$ wild type when either Ca^{2+} or Mg^{2+} (2.5 mM) was added to the medium (Fig. 3C).

Together, these results showed that destabilization of the Δ*ail* membrane can be relieved by the addition of glucose, glycerol, Ca^{2+}, or Mg^{2+} to the medium.

Analysis of proteins released by *Y. pestis* Δ*ail* mutant during early stationary growth phase at 37°C further defined the phenotype as lacking Caf1 capsule. Tandem mass spectrometry (MS/MS) analysis of the supernatant from the Δ*ail* mutant identified catabolic and anabolic enzymes, heat shock and stringent response components, and ribosomal proteins, indicating generalized cell lysis (Table 2). Specifically lacking were phage, pesticin, and Caf1 capsule proteins. Bacterial cell lysis can result from prophage or bacteriocin induction (43–45), and the MS/MS data indicated that these processes were not involved in lysis of the *Y. pestis* Δ*ail* mutant. Consistent with this interpretation was that phage particles were not observed in TEM images (Fig. 1C and 2 and data not shown), and plaques were not generated from these supernatants on other *Y. pestis*, *Y. enterocolitica*, or *Y. pseudotuberculosis* strains (data not shown). To confirm that pesticin was not involved in Δ*ail* mutant lysis, a deletion of *pst* was engineered, and there was no difference ($P = 0.53$, Student's *t* test) in lysis between the Δ*ail* ($1.9 \times 10^7 \pm 0.6 \times 10^7$ CFU/ml) and the Δ*ail* Δ*pst* ($2.9 \times 10^7 \pm 0.9 \times 10^7$ CFU/ml) double deletion mutants.

The lack of Caf1 in the supernatant, normally produced and assembled on the cell surface at 37°C, was further investigated by immunofluorescence of bacterial cells. The Δ*ail* mutant had no cell surface capsule protein (Fig. 4). However, if glucose was added to the medium, it reversed this effect, just as glucose inhibited lysis (Fig. 4 and 3A).

Together, these results showed that Δ*ail* mutant lysis was not due to induction of prophage or pesticin and identified loss of capsule production as a new Δ*ail* mutant phenotype.

Lysis of *Y. pestis* Δ*ail* mutant at 37°C was suppressed by mutations in the phospholipase A gene, *pldA*. The inhibition of the Δ*ail* mutant lytic phenotype implied suppressor mutations could be found. A transposon screen of the Δ*ail* mutant employing a mini-Tn*5lacZ* revealed several independent isolates that did not exhibit cell lysis, maintained high absorbance at the optical density at 600 nm (OD_{600}), and had no decrease in cell viability when incubated at 37°C (data not shown). The transposon insertions each mapped to different sites within *pldA* (phospholipase A), an enzyme required to maintain phospholipid asymmetry in the OM under stress conditions (3, 6).

To confirm the role of PldA in Δ*ail* mutant lysis, a *pldA* deletion was constructed by site-directed mutagenesis. The *Y. pestis* Δ*ail* Δ*pldA* mutant lost the lytic phenotype, as determined by (i) decreased protein release into the supernatant (Fig. 5A), (ii) sustained stationary-phase viability similar to that of the KIM6$^+$ wild type (Fig. 5B), and (iii) maintained absorbance at OD_{600} (data not shown). To further show that the role of PldA in lysis of the Δ*ail* mutant was due to enzymatic activity, the site-specific catalytic mutants PldA^{S164A} and PldA^{WT} were expressed in *trans* in the *Y. pestis* Δ*ail* Δ*pldA* mutant. The strains were compared for growth and lysis in stationary phase (48 h), as defined by protein release into culture supernatants. There was no difference in growth rate between the Δ*ail* Δ*pldA*, Δ*ail* Δ*pldA* (pPldA^{WT}), and Δ*ail* Δ*pldA* (pPldA^{S164A}) strains during logarithmic phase (data not shown). However, complementation with enzymatic PldA (pPldA^{WT}) restored the lysis phenotype, unlike complementation with inactive PldA (pPldA^{S164A}) (Fig. 5C).

Together, these results showed that suppressing PldA activity prevented lysis of the Δ*ail* mutant at 37°C and correlates with the phospholipid changes measured in this mutant.

Downregulation of *pldA* expression occurred at 37°C and was further decreased by glucose or Ca²⁺. Because a deletion of *pldA* reversed the temperature-sensitive lytic phenotype of the Δ*ail* mutant, *pldA* regulation was investigated. The *Vibrio harveyi lux* operon transcriptional reporter system was placed under the control of the *Y. pestis* Kim6$^+$ *pldA* promoter. The effects of temperature and glucose or Ca²⁺ on *pldA-lux* expression were assayed, analyzed with a two-way analysis of variance (ANOVA), and found to be different (Fig. 6). Based on *pldA* suppressor results (Fig. 5), the simplest prediction was that *pldA* expression would be higher at 37°C in the Δ*ail* mutant background than that for the Δ*ail* mutant at 28°C. Contrary to this expectation, the overall levels of *pldA* expression were lower at 37°C than 28°C (Fig. 6) for all strains, including

TABLE 2 Supernatant proteins released by *Y. pestis* KIM6$^+$ Δ*ail* mutant during early stationary growth phase at 37°C

Gene ID	ORF	Product	Function	No. of peptides[a]	Protein coverage[b] (%)
y0870	katG	Catalase peroxidase	Protection responses: detoxification	12	24.9
y1004	tauA	Lipoprotein	ABC-type nitrate/sulfonate/bicarbonate transport systems	4	25.6
y1098	caf1M	F1 chaperone protein	Chaperones	3	18.2
y3165	ptr	Protease III precursor	Degradation of proteins, peptides	3	5.2
y3140	dapD	2, 3, 4, 5-Tetrahydropyridine-2,6-dicarboxylate N-succinyltransferase	Amino acid biosynthesis: lysine	3	13.5
y2629	gnd	6-Phosphogluconate dehydrogenase	Energy metabolism, carbon: oxidative branch, pentose pathway	3	9.5
y1990	tpx	Thiol peroxidase	Protection responses: detoxification	3	31.1
y1968	gst	Glutathionine S transferase	Biosynthesis of cofactors, carriers: thioredoxin, glutaredoxin, glutathione	3	13.4
y1489	cysK	Cysteine synthase A	Amino acid biosynthesis: cysteine	3	17.4
y3986	tufB	Elongation factor Tu	Proteins–translation and modification	2	9.1
y3310	tktA	Transketolase	Central intermediary metabolism: nonoxidative branch, pentose pathway	2	4.1
y2756	pepN	Aminopeptidase N	Degradation of proteins, peptides	2	2.9
y0814	eno	Phosphopyruvate hydratase	Energy metabolism, carbon: glycolysis	2	6.7
y0769	lpdA	Dihydrolipoamide dehydrogenase	Energy metabolism, carbon: E3 component of pyruvate and 2-oxoglutarate dehydrogenase complex	2	6.7
y0609	mopA	Chaperonin GroEL	Chaperones	2	7.7
y0464	fadB	Multifunctional fatty acid oxidation complex subunit alpha	Degradation of small molecules; fatty acids	2	4.5
y0444	udp	Uridine phosphorylase	Salvage of nucleosides and nucleotides	2	14.2
y0360	trxA	Thioredoxin 1	Biosynthesis of cofactors; carriers: thioredoxin, glutaredoxin, glutathione	2	23.1
y1069	ymt	Murine toxin	Lipid metabolism	1	3.4
y4135	atpD	F0F1 ATP synthase subunit beta	ATP-proton motive force interconversion	1	3.9
y4080	sodA	Superoxide dismutase	Protection responses: detoxification	1	6.8
y4004	rplF	50S ribosomal protein L6	Structural component; ribosomal proteins–synthesis, modification	1	7.9
y3985	fusA	Elongation factor G	Proteins–translation and modification	1	2.0
y3977	fkpA	FKBP-type peptidyl-prolyl cis-trans isomerase	Proteins–translation and modification	1	4.7
y3938	rpe	Ribulose-phosphate 3-epimerase	Central intermediary metabolism: nonoxidative branch, pentose pathway	1	6.1
y3855	prlC	Oligopeptidase A	Degradation of proteins, peptides	1	1.5
y3712	talB	Transaldolase B	Central intermediary metabolism: nonoxidative branch, pentose pathway	1	3.5
y3308	pgk	Phosphoglycerate kinase	Energy metabolism, carbon: glycolysis	1	4.4
y3135	tsf	Elongation factor Ts	Proteins–translation and modification	1	6.0
y3073	grpE	Heat shock protein GrpE	Posttranslational modification, protein turnover, chaperones	1	7.3
y3069	sdhA	Succinate dehydrogenase flavoprotein subunit	Energy metabolism, carbon: TCA cycle	1	2.4
y2855	grxA	Glutaredoxin 1	Carrier; biosynthesis of cofactors, carriers: thioredoxin, glutaredoxin, glutathione	1	12.6
y2735	ompA	Outer membrane protein A	Outer membrane constituents	1	3.6
y2266	argS	Arginyl-tRNA synthetase	Aminoacyl-tRNA synthetases, tRNA modification	1	2.3
y2246	pykA	Pyruvate kinase	Energy metabolism, carbon: glycolysis	1	2.5
y2165	gapA	Glyceraldehydes-3-phosphate dehydrogenase	Energy metabolism, carbon: glycolysis	1	4.2
y2063	acnA	Aconitate hydratase	Energy metabolism, carbon: TCA cycle	1	1.5
y1953		Hypothetical protein	Unknown; belongs to glutaredoxin (GRX) family	1	10.7
y1802	icdA	Isocitrate dehydrogenase	Energy metabolism, carbon: TCA cycle	1	3.5
y1507		Putative aminotransferase	Amino acid biosynthesis: alanine	1	3.9

TABLE 2 (Continued)

Gene ID	ORF	Product	Function	No. of peptides[a]	Protein coverage[b] (%)
y1485	crr	Glucose specific PTS system component	Transport of small molecules; carbohydrates, organic acids, alcohols	1	8.3
y1027	clpP	ATP dependent Clp protease proteolytic subunit	Degradation of proteins, peptides	1	9.2
y1001	ribH	Riboflavin synthase subunit beta	Biosynthesis of cofactors, carriers: riboflavin	1	12.2
y0988		Putative peroxidase	Protection responses: detoxification	1	5.5
y0960	pepD	Aminoacyl-histidine dipeptidase	Degradation of proteins, peptides	1	2.9
y0947	gmhA	Phosphoheptose isomerase	Surface polysaccharides and antigens	1	13.0
y0815	sodC	Superoxide dismutase	Protection responses: detoxification	1	12.8
y0767	aceE	Pyruvate dehydrogenase subunit E1	Energy metabolism, carbon: pyruvate dehydrogenase	1	1.5
y0668	mdh	Malate dehydrogenase	Energy metabolism, carbon: TCA cycle	1	3.5
y0635	purA	Adenylosuccinate synthetase	Purine ribonucleotide biosynthesis	1	2.8
y0510	acs	Acetyl-CoA synthetase	Fatty acid and phosphatidic acid biosynthesis	1	1.8
y0480	rplK	50S ribosomal protein L11	Structural component; ribosomal proteins - synthesis, modification	1	9.9
y0477	tufB	Elongation factor Tu	Proteins - translation and modification	1	4.8
y0392		Hypothetical protein	Unknown; potential TIM-barrel signal transduction protein	1	7.5
y0163		Hypothetical protein	Unknown	1	9.2
y0132	sspA	Stringent starvation protein A	Regulator of transcription; a RNA polymerase-associated protein	1	6.6
y0125		Isoprenoid biosynthesis protein	Unknown; putative factor	1	12.4
y0024	pgi	Glucose-6-phosphate isomerase	Energy metabolism, carbon: glycolysis	1	2.9
y0016	aceA	Isocitrate lyase	Central intermediary metabolism: glyoxylate bypass	1	3.4

[a]Number of peptides identified for indicated protein.
[b]Peptide coverage (%) of indicated protein.

the Δ*ail* mutant, with a 7.8-fold decrease in the KIM6$^+$ wild type and 4.3-fold decrease in Δ*ail* mutant and Δ*ail*/Δ*ail*$^+$ complemented strain ($P < 0.0001$, one-way ANOVA, Tukey's honestly significant difference [HSD]). It is noteworthy that under these temperature conditions the Δ*ail/ail*$^+$ complemented strain had increased *pldA* expression compared to the KIM6$^+$ wild type and was similar to the Δ*ail* mutant.

Interestingly, glucose in the medium completely repressed *pldA* expression in all strains at 37°C ($P < 0.0001$, one-way ANOVA, Tukey's HSD) (Fig. 6). The complete inhibition of *pldA* expression and lysis (Fig. 3) by glucose may provide insights into the mechanism of its suppressive effects. Addition of Ca^{2+} to the medium also repressed *pldA* but to a lesser extent than glucose. Ca^{2+} had an average fold decrease of 2.5 in *pldA* expression in all strains (Fig. 6).

Together, these results showed that *pldA* expression was temperature, glucose, and Ca^{2+} dependent. Glucose and, to a lesser extent, Ca^{2+}, significantly repressed *pldA* expression, consistent with the suppression of lysis at 37°C in the Δ*ail* mutant and in Δ*ail* mutant strains with *pldA* mutations. Lower levels of *pldA* expression at 37°C versus 28°C suggest that thermosensitive PldA-dependent lysis of the Δ*ail* mutant is defined by the availability of PldA substrates in the OM outer leaflet rather than the PldA concentration.

Expression of the heat shock sigma factor promoters *rpoE* and *rpoH* was decreased in the *Y. pestis* Δ*ail* mutant at 37°C. Lysis of the Δ*ail* mutant at 37°C, and not at lower temperatures, reflected its thermosensitivity. In addition, heat shock factors GroEL, PrlC, and GrpE were released into the medium at 37°C (Table 2). Thus, the expression of two sigma factors, RpoE and RpoH, that regulate the extracytoplasmic and cytoplasmic heat shock responses (46), respectively, was investigated. The *Vibrio harveyi lux* operon transcriptional reporter system was placed under the control of the *Y. pestis* KIM6$^+$ *rpoE* or *rpoH* promoters. KIM6$^+$ wild type, the Δ*ail* mutant, and Δ*ail/ail*$^+$ complemented strain with the *lux* constructs were grown to mid-logarithmic phase at 28°C or 37°C, and luminescence was measured.
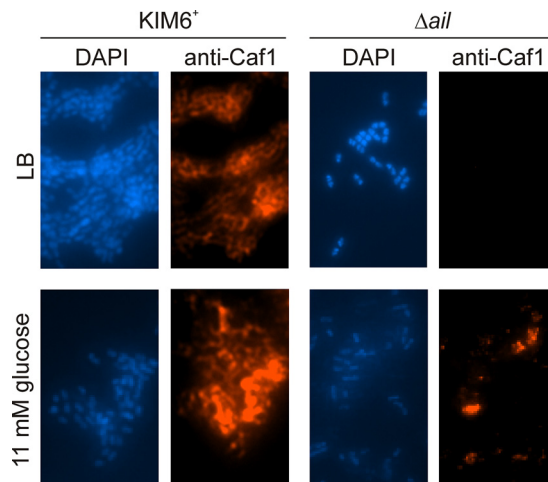
FIG 4 *Y. pestis* Δ*ail* mutant had no cell surface capsule protein (Caf1) unless glucose was added to the medium. *Y. pestis* KIM6+ wild type and the Δ*ail* mutant were grown with aeration to mid-logarithmic phase at 37°C in Luria-Bertani (LB) broth with or without 11 mM glucose. Cells were centrifuged, washed with PBS, and heat fixed on glass slides. *Y. pestis* cells (blue) were stained with DAPI, and Caf1 protein (red) was detected with mouse anti-Caf1 followed by goat anti-mouse Alexa Fluor 546 antibodies. Cells are at ×1,000 magnification and are representative of more than 20 microscopic fields.

There was no induction of *rpoE* at 37°C above levels observed at 28°C (Fig. 7A) in the Δ*ail* mutant; expression of *rpoE* in the Δ*ail* mutant was 3-fold lower than that in the KIM6+ wild-type and Δ*ail*/*ail*+ strains during growth at elevated temperature (Student's *t* test, $P < 0.001$). Both KIM6+ wild-type and Δ*ail*/*ail*+ complemented strains increased *rpoE* expression at 37°C compared to 28°C (Student's *t* test, $P < 0.001$). In contrast, a small decrease (Student's *t* test, $P < 0.01$) in *rpoE* expression in the Δ*ail* mutant was observed at elevated temperature (Fig. 7A). Decreased levels of *rpoE* expression in the Δ*ail* mutant versus
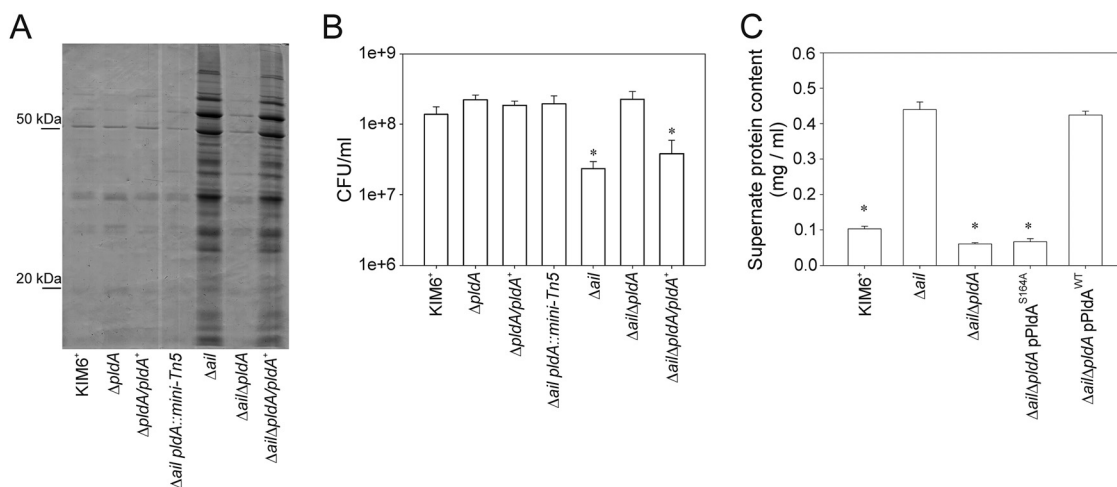

FIG 5 Mutations in the phospholipase A gene, *pldA*, suppressed lysis of *Y. pestis* Δ*ail* mutant at 37°C. *Y. pestis* KIM6+ wild type, the Δ*ail* mutant, the Δ*pldA* mutant, the catalytic site-specific PldA^S164A mutant, complemented strains, and the indicated double mutants were grown with aeration to late stationary phase (24 h/37°C) in Luria-Bertani (LB) broth. (A) Cell-free supernatants from cultures were ethanol precipitated, separated by 12.5% SDS-PAGE, and stained with Coomassie blue. Protein bench mark standard positions are indicated on the left. Only the wild type or strains carrying *pldA* mutations did not release increased amounts of protein into the supernatants. (B) Strains were grown as described above for 48 h and CFU numbers determined by plate count. Only the wild type or strains carrying a *pldA* mutation did not lyse. (C) The protein contents of cell-free supernatants from the catalytic site-specific PldA^S164A mutant and control cultures were quantified by Bradford assays. Only strains with an enzymatic phospholipase A (PldA) had increased amounts of protein released into the supernatants by *Y. pestis* Δ*ail* mutant. Results are means ± SE from two assays performed in duplicate on separate days; asterisks indicate significant difference by ANOVA ($P < 0.05$).
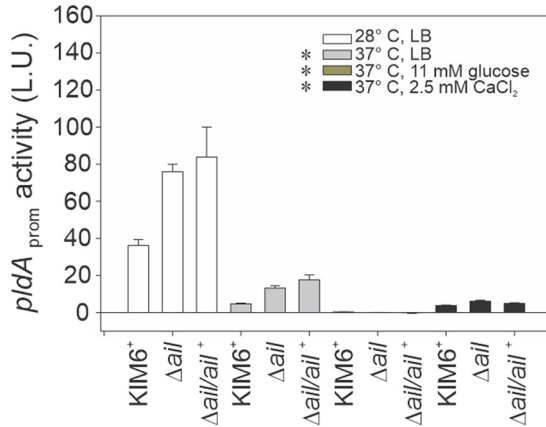
FIG 6 Expression of *pldA* was repressed at 37°C and further decreased by glucose or Ca^{2+}. *Y. pestis* KIM6⁺ wild type, the Δ*ail* mutant, and the Δ*ail/ail*⁺ complemented strain were transformed with the *lux* operon reporter under the control of the *Y. pestis pldA* promoter. Cells were grown with aeration to an OD_{600} of 1.0 at 28°C or 37°C in Luria-Bertani (LB) broth with or without 11 mM glucose or 2.5 mM $CaCl_2$. Expression was measured spectrophotometrically as luminescence activity units (L.U.). Growth with glucose or Ca^{2+} repressed *pldA* expression at 37°C. Results are means ± SE from at least two assays performed in triplicate on separate days; an asterisk indicates significant difference between the growth conditions (two-way ANOVA, $P < 0.05$).

KIM6⁺ wild-type and Δ*ail/ail*⁺ strains were also found at 28°C, but the difference was small (average of 1.2-fold; Student's *t* test, $P < 0.01$).

A similar pattern was observed in *rpoH* regulation (Fig. 7B); there was no induction of *rpoH* at 37°C in the Δ*ail* mutant. While *rpoH* activation increased 1.8-fold in KIM6⁺ wild-type and Δ*ail/ail*⁺ strains at 37°C (Student's *t* test, $P < 0.01$), no statistical difference was observed between *rpoH* levels at 28°C and 37°C in the Δ*ail* mutant. The Δ*ail* mutant also showed lower levels of expression than KIM6⁺ wild-type and Δ*ail/ail*⁺ strains at 28°C. Altogether, these data indicated that deletion of *ail* suppressed the induction of two critical heat shock response sigma factors and showed Ail to be a key signaling component of the *Y. pestis* thermoregulatory system.

In the well-studied *E. coli* RpoE-induced responses, DegP is a periplasmic chaperone and protease essential for growth and viability at higher temperatures (47). The protein reduces the rate of misfolded and denatured proteins present in the periplasmic space and, thus, alleviates extracytoplasmic stress. The inability to rescue the Δ*ail* mutant from lysis by overexpression of either DegP or its protease-deficient mutant, DegP[S210A] (data not shown), suggested that lysis was not due to compromised maturation of the
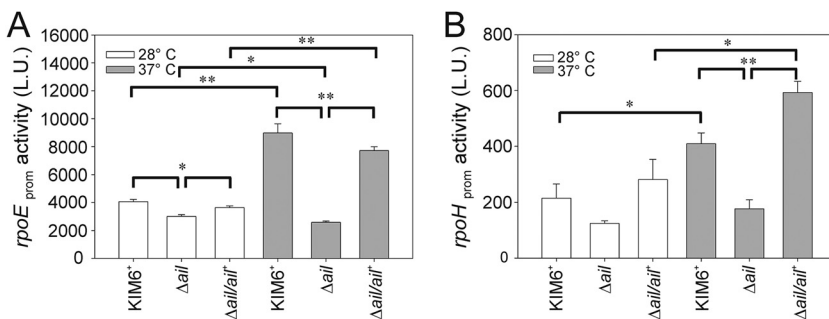

FIG 7 Expression of the heat shock sigma factor promoters *rpoE* and *rpoH* was decreased in the *Y. pestis* Δ*ail* mutant at 37°C. *Y. pestis* KIM6⁺ wild type, the Δ*ail* mutant, and the Δ*ail/ail*⁺ complemented strain were grown with aeration to an OD_{600} of 1.0 at 28°C or 37°C in Luria-Bertani (LB) broth. Each strain was transformed with the *lux* operon reporter under the control of the *Y. pestis rpoE* (A) or *rpoH* (B) promoter. Expression was measured spectrophotometrically as luminescence activity units (L.U.). Results are means ± SE from at least three assays performed in triplicate on separate days; an asterisk indicates $P < 0.05$, and a double asterisk indicates $P < 0.001$ (Student's *t* test).

OM proteome. To assess if induction of other RpoE regulon components could suppress lysis, an *E. coli* H198PDegSΔPDZ protein was expressed in the Δ*ail* mutant. DegS is a serine endoprotease that activates RpoE by releasing it from the inner membrane in response to the presence of misfolded OMPs in periplasmic space. The mutation H198P and deletion of the PDZ domain stabilize its active form and increase its catalytic activity (41). Preliminary results showed that even though *rpoE* expression in the Δ*ail* mutant at 37°C increased by only 2-fold (see Fig. S1A in the supplemental material), contrary to our expectations, this strain showed enhanced lysis instead of inhibition (Fig. S1B). This DegS enhanced lysis phenotype was inhibited in the Δ*ail* Δ*pldA* background, and luminescence showed that *pldA* expression was not part of the RpoE regulon (Fig. S1B and C). These data indicated that lysis of the Δ*ail* mutant was regulated by components of the RpoE regulon involved in lipid homeostasis rather than protein stability.

DISCUSSION

The most important finding of this study was that the deletion of *Y. pestis ail*, encoding a single OMP, resulted in significant, and not previously described, pleiotropic effects. These effects included a temperature-sensitive lysis due to membrane destabilization, lack of capsule assembly, and disruption of stress response signaling associated with nutrient deprivation and temperature changes. The lytic phenotype could be suppressed physiologically by supplementation of growth media with glucose, glycerol, or cations or genetically by mutations in *pldA*. Together, these results indicate loss of a major OMP, until now primarily associated with virulence, can also have significant implications in cell signaling and growth. A model summarizing this complex system is shown in Fig. 8.

The Ail-associated lytic phenotype is temperature dependent and Ail specific. It was not recognized previously because the conditions used in studies examining Ail contributions to virulence (11) employed *Y. pestis* pCD1$^+$ strains. This fact had several ramifications. First, all three human-pathogenic strains of *Yersinia* have the unique phenotype of being calcium dependent (2.5 mM) for growth at 37°C, conditions shown here to suppress lysis. This phenotype, referred to as the low calcium response, is pCD1 virulence plasmid mediated. Second, the virulence plasmids in pathogenic *Yersinia* are unstable at 37°C, so cultures were consistently grown at lower temperatures to ensure the plasmid was not lost. Therefore, *Y. pestis* pCD1$^+$ Δ*ail* mutant strains were grown at 28°C to mid-logarithmic growth phase before conducting animal or mammalian cell culture studies at 37°C. If grown at 37°C, *Y. pestis* pCD1$^+$ Δ*ail* mutants were supplemented with Ca^{2+}. Therefore, the three parameters of low-temperature growth, growth to mid-logarithmic phase, and growth of cells supplemented with Ca^{2+} at 37°C were conditions that masked detection of the Δ*ail* lytic phenotype.

Regarding the specificity of Ail, overexpression of the other three *Y. pestis* Ail homologs did not compensate for the loss of Ail, indicating Ail has a specific stabilizing effect when cells are shifted to 37°C. Only complementation with *ail* stabilized the membrane. A possible role of Ail in maintaining OM homeostasis could be regulation of PldA activity via direct protein-protein interaction or sequestration of membrane-damaging products through bridging with LPS molecules, phospholipids, or both. In *E. coli*, recently discovered interactions between OmpC and the Mla PL transport system suggest that OMPs can specifically facilitate PL transport between the OM and inner membrane (48, 49). It will be interesting to determine if the deletion of *ail* homologs in other Gram-negative bacteria shows a similar phenotype. No reports indicating lysis of *ail* deletions for *Y. enterocolitica* or *Y. pseudotuberculosis* have been reported but may have been missed due to routine Ca^{2+} supplementation required for growth at 37°C. Thus, this phenotype may be unique to pathogenic *Yersinia* and suggests that the physicochemical properties of *Yersinia* LPS at 37°C, with decreased acylation of lipid A, are a unique contributing factor.

To detect changes in membrane permeability in the Δ*ail* mutant, antibiotic sensitivity was determined to (i) vancomycin, not normally active against Gram-negative
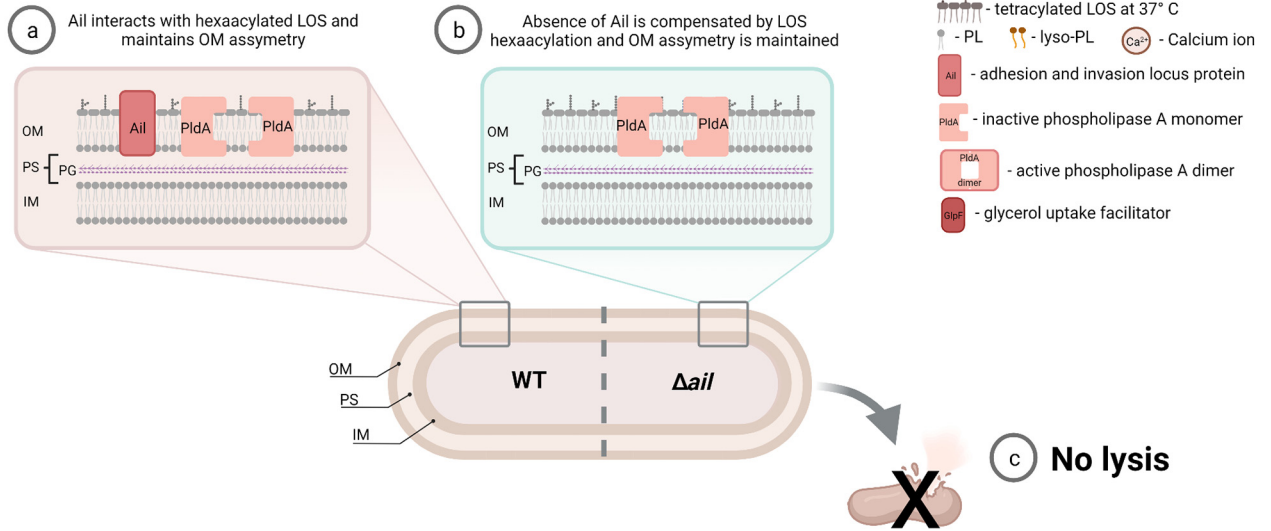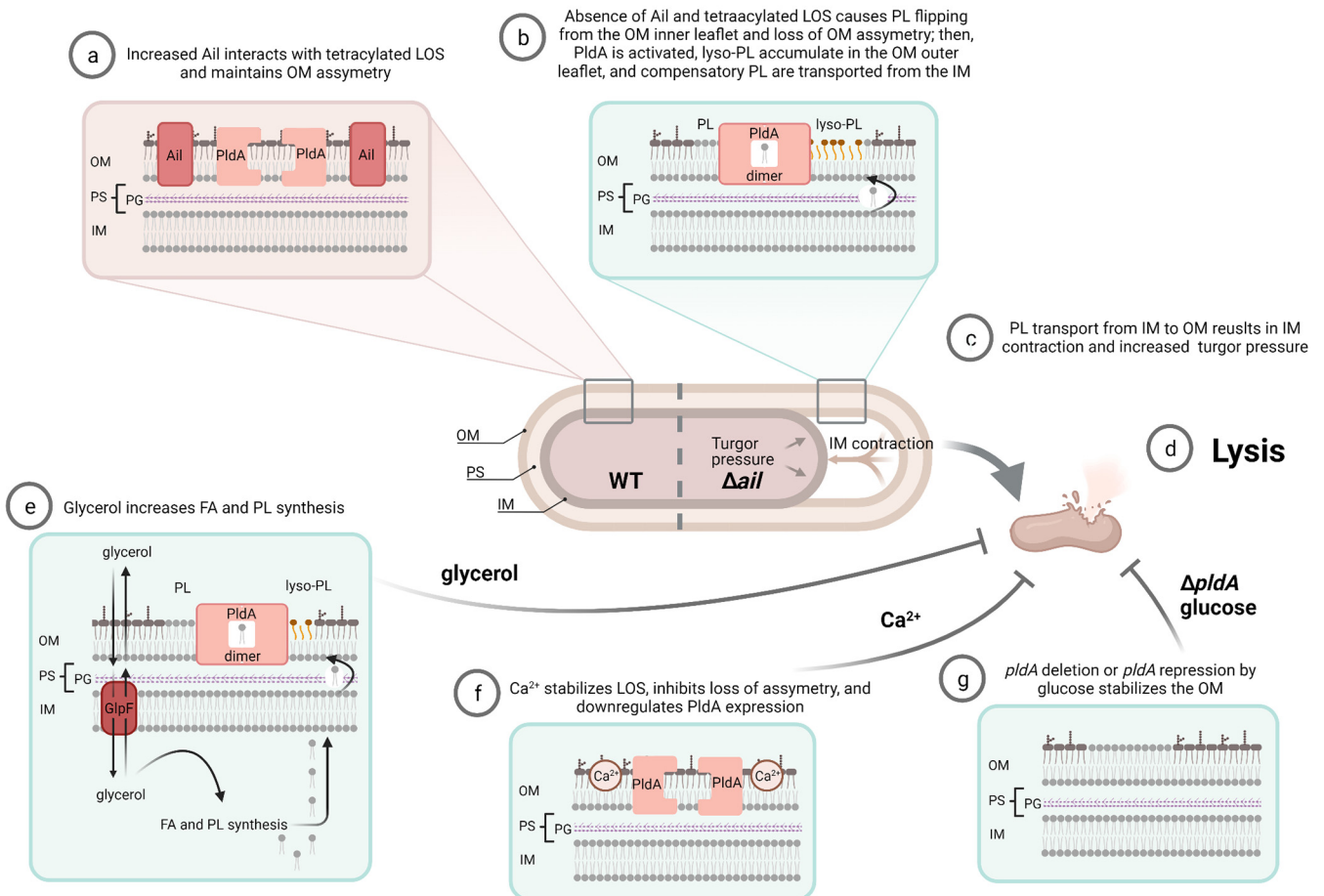
FIG 8 Model of temperature-dependent Ail contribution to OM stabilization. Panel I shows conditions for maintaining OM asymmetry and cell lysis prevention at ambient temperature. Panel II, a, b, and c, compares the wild type and the Ail mutant for OM disruption and cell lysis at mammalian temperature. Panel II, d, e, and f, shows conditions that suppress cell lysis. OM, outer membrane; PS, periplasmic space; PG, peptidoglycan; IM, inner membrane; LOS, lipooligosaccharide; PL, phospholipid; lyso-PL, lysophospholipid; FA, fatty acid. Figure created with BioRender.com.

bacteria due to the vancomycin-impermeable OM barrier (50); (ii) novobiocin, an indicator of the OM permeability to hydrophobic compounds (51); and (iii) polymyxin B, an antibiotic known to bind to LPS through both ionic and hydrophobic interactions (52). An increased sensitivity was found only to polymyxin B. This supports that the Δail mutant membrane was defective in LOS structure, PL structure, or their concentrations. Polymyxin B sensitivity of $Y.\ pestis\ ail$ site-directed mutants was also reported by Singh et al. (25), and these authors mapped polymyxin B sensitivity to base cluster II residues of Ail, a region that makes direct contact with LOS. Surprisingly, the Δail mutant showed decreased sensitivity to SDS detergent. Less protein in the OM due to deletion of ail should expose more PL and a predicted increased sensitivity to anionic detergents. The fact that cells were more resistant to SDS is unexplained.

The 37°C temperature-dependent lysis phenotype of the Δail mutant manifests as cells enter stationary phase. Although observable release of cellular components occurred during the logarithmic phase of growth, profound morphological deterioration was not observed until stationary phase. Electron micrographs of cells at this stage show decreased cytoplasmic volume and inner membrane surface area, suggesting that cells are losing membrane faster than new PL can be synthesized. Previously reported temperature- and growth phase-dependent increased expression of proteins involved in fatty acid import ($fadL$) and catabolism ($fadI$, $fadB$, $faoA$, and $yafH$) (53, 54) suggest that $Y.\ pestis$ preferentially uses lipids as an energy source at 37°C in stationary phase. Preliminary MS analysis of bacterial PL content showed differences for some PL peaks between the Δail mutant and wild-type cells. These differences were reduced when cells were grown in LB broth supplemented with glycerol. Whether PldA activity is specific or if glycerol leads to synthesis of stabilizing PL species needs more investigation. Genes regulating glycerol uptake ($glpF$) and metabolism ($glpK$ and $glpD$) are upregulated at 37°C (54). Importantly, glucose drastically reduced expression of $pldA$, consistent with reduced cell lysis that required PldA activity. Therefore, supplementing media with glycerol or glucose, substrates that can promote lipid biosynthesis and suppress $pldA$ expression, rescued cells from stationary-phase death.

Physiological suppression of lysis was also achieved by supplementing LB broth with Mg^{2+} or Ca^{2+} cations. Mg^{2+} levels are very low in LB broth (55). Ca^{2+} interacts with negatively charged LPS molecules and anionic PLs to stabilize the OM. Clifton et al. show, in a synthetic Gram-negative OM model, that removal of calcium results in a dramatic 20% mixing of LPS and PL between the inner and outer leaflet bilayers to stabilize repulsive electrophoretic forces (56). Suppression of lysis, evidenced by wild-type-level concentrations of proteins in culture supernatants, demonstrated this stabilizing effect of Ca^{2+} on OM stability. Mg^{2+} levels had an effect nearly identical to that of Ca^{2+}. The expression of $pldA$ was repressed by Ca^{2+}. In addition, nuclear magnetic resonance (NMR) studies by Singh et al. (25) show that there is direct Ail interaction with LPS to stabilize the OM. It is likely that, here, divalent cations compensated for Ail loss, as predicted in the Clifton (56) model, by preventing PL translocation between the OM inner and outer leaflets. We concluded that excess divalent cations are necessary and sufficient to suppress the Δail mutant lysis phenotype.

$Y.\ pestis$ synthesizes a capsule at 37°C comprised of the Caf1 protein. This protein was conspicuously missing in cell supernatant proteins released by the Δail mutant grown at 37°C and could not be detected by immunofluorescence with Caf1 antibody. Membrane stabilization provided by glucose supplementation to LB broth restored capsule formation at 37°C in the Δail mutant. This indicated loss of Ail in the OM had a disruptive effect on additional proteins. Loss of Caf1 is also consistent with the reports that a Δail mutant shows increased immune infiltration and phagocytosis in lymph tissue of infected rodents (26, 28). Although the lytic phenotype of the Δail mutant in $vitro$ may alter virulence, the previously described Ail-mediated serum resistance is a major contributor to the high mortality of $Y.\ pestis$ (11). Low virulence of the Δail mutant in a pneumonic model of plague correlates with a high potential of rat serum to kill the Δail cells. This trait is not observed with mouse serum, and there is no decrease

in virulence in the mouse model (11). In addition, the combined blood glucose and calcium concentrations are sufficient to inhibit lysis of the Δ*ail* mutant *in vivo* (57).

The OM of the Gram-negative bacterium is the primary barrier against the harsh extracellular environment (1), so any disturbances in this membrane are counteracted by the cell to maintain barrier integrity. Under normal conditions, PL is excluded from the outer leaflet of the OM. However, in response to certain extracytoplasmic stress conditions, Gram-negative bacteria can accumulate PL in the outer leaflet of the OM to maintain membrane continuity (1, 2, 5). Incorporation of PL into the OM ensures OM integrity, but its selectivity and overall stability is impaired by formation of PL patches that are more permeable to small toxic molecules (1). PL in the OM activate mechanisms to regain the OM asymmetry. For example, in *E. coli*, the PL present in the OM outer leaflet are removed by two enzymes: the OM β-barrel PldA (3, 6) and OM β-barrel lipid A palmitoyl transferase (PagP) (58). Upon activation by mislocalized PL present in the OM outer leaflet, PldA catalyzes hydrolysis of PL or lyso-PL and removes a fatty acid residue to restore asymmetry (6). PagP acylates lipid A using a palmitate chain from an outer leaflet PL donor (59), and its expression is induced in response to the limitation of divalent cations (60). PagP activity increases heptaacylated lipid A by this palmitate addition.

The *Y. pestis* response to these conditions is different from that of *E. coli*. Acylation of lipid A is thermoregulated in *Y. pestis* and is the major LOS structural change between these two temperatures. Due to deletion of *lpxL* (14) and a point mutation in *pagP* (13), *Y. pestis* lipid A is predominantly tetraacylated at 37°C. It is interesting that *lpxL* null mutants in *E. coli* are conditionally lethal at temperatures above 33°C for reasons that are unclear (61). One speculation is incorporation of unsaturated palmitoleic acid in *lpxL*-null mutants is detrimental to growth at higher temperatures due to its effect on the fluidity of the membrane (62). Temperature-sensitive mutants of *lpxL* also show an abnormally high ratio of PL to protein in the OM when grown at elevated temperature. Perhaps to compensate for the deletion of *lpxL*, *Y. pestis* requires compensatory mutations for high-temperature growth, such as elevated expression of Ail, to stabilize the OM at 37°C. Thus, the loss of Ail in the OM may unmask the instability of tetraacylated lipid A at 37°C. Restoration of hexaacylation of *Y. pestis* lipid A by restoration of *lpxL* or *pagP* may compensate for the loss of Ail.

The phenotype of the *Y. pestis* Δ*ail* mutant is remarkably like the phenotype of the *E. coli* dominant mutation in *mlaA** (maintenance of lipid asymmetry) reported by Sutterlin et al. (4). The *mlaA** mutation results in increased OM permeability, blebbing in log phase, and cell lysis when cells transition to stationary growth phase. This conditional lethal mutation can be rescued by Mg^{2+} and Ca^{2+}, lipid supplementation to LB broth, or by a suppressor mutation in *pldA*. Sutterlin et al. hypothesize that the *mlaA** allele increases the transfer of PL from the inner to outer leaflet of the OM (a reversal of MlaA normal activity). This aberrant flow of PL into the outer leaflet activates PldA. Whether this model applies to *Y. pestis* is worth further examination.

While heat shock is underexplored in *Y. pestis*, the demonstration that deletion of Ail disrupted both RpoH and RpoE responses is significant. RpoE maintains cell envelope homeostasis by governing expression of multiple genes regulating OM protein components and genes regulating fatty acid, PL, and LPS components (63–65). The inability to rescue cells from lysis by overexpressing *rpoE*-controlled DegP or its protease-deficient mutant (both reduce misfolded proteins) is consistent with the loss of Ail primarily disrupting OM lipid asymmetry and not OM proteome stability. The overexpression of H198P DegSΔPDZ, which led to constitutive *rpoE* expression in the *Y. pestis* Δ*ail* mutant and induction of genes affecting membrane stability, increased lysis rather than rescue. Similarly, in *E. coli*, *rpoE* is induced in stationary phase, but if overexpressed, it leads to cell lysis (66–68). The fact that DegS-enhanced lysis was suppressed in the Δ*ail* Δ*pldA* mutant also indicates that Ail and PldA are central to maintaining regulation of PL turnover and that unconstrained RpoE levels lead to lethal increases in this rate. Our data and that of others (53) show that increased expression of *rpoE* at 37°C versus 28°C inversely

correlates with *pldA* expression in wild-type *Y. pestis* KIM6$^+$. Because *pldA* was not a part of the RpoE regulon based on the *lux*-reporter fusion constructs, it will be interesting to identify indirect modes of RpoE regulation of PldA-dependent lysis. These results showed the interplay between heat shock systems, OMP, and lipids are integral to maintain OM integrity at elevated temperatures.

This work supports the structural characterization of Ail-LOS interactions in NMR models (25, 69). It also supports the broad context of lipid flow between membranes in other Gram-negative bacteria, demonstrated by the laboratories of Silhavy and Trent (4, 9). *Y. pestis* is an effective pathogen because of its genome reduction, but loss of *lpxL* and *pagC* have significant fitness costs if the protein content of the membrane is disturbed. Much of the work on protein-lipid interactions in the membrane has centered on the role of lipids generating a stable environment for protein function. Less attention has been paid to the converse that proteins provide a stable environment for membrane lipids. The contribution of Ail to *Y. pestis* membrane integrity illustrates this point.

MATERIALS AND METHODS

Media, strains, and primers. Bacteria were cultured in low-salt LB broth (Luria-Bertani or lysogeny broth) (70). Congo red agar plates were used to screen for the presence of the *Y. pestis* pCD1 virulence plasmid (71). Antibiotics were used at the following concentrations: nalidixic acid (Nal), 50 μg ml^{-1}; chloramphenicol (Cm), 30 μg ml^{-1}; ampicillin (Amp), 100 μg ml^{-1}; and kanamycin (Kn), 50 μg ml^{-1}. Cultures were supplemented with 1 mM isopropyl-β-D-1-thiogalactopyranoside (IPTG) for induction of Ail and its homologues, DegP, DegP^{S210A}, and H198PDegSΔPDZ. LB agar plates with Cm and Nal or cefsulodin-irgasan-novobiocin (CIN) *Yersinia* selective plates (BD, Franklin Lakes, NJ) with Cm were used to select single-crossover recombinants. LB agar plates with 5% sucrose and lacking NaCl were used to select double-crossover recombinants during targeted gene deletion that employed the *sacBR* locus encoding levensucrase, as described previously (11, 24). In some experiments, LB medium was supplemented with 11 mM glucose, 11 mM ribose, 11 mM xylose, 11 mM sorbitol, 22 mM or 44 mM glycerol, 2.5 mM calcium chloride, or 2.5 mM magnesium chloride. Tables 3, 4, and 5 list strains, plasmids, and primers, respectively. Only one deletion of *ail* was used with or without the Kn cassette (*Y. pestis* KIM6$^+$ Nal^r Δ*ail*::*npt* or *Y. pestis* KIM6$^+$ Nal^r Δ*ail*) and is referred to throughout as the Δ*ail* mutant.

Bacterial growth measurements. Inocula from overnight cultures grown at 28°C in LB broth with aeration were diluted into fresh prewarmed LB broth, and incubation was continued at 37°C. A Beckman Coulter DU530 spectrophotometer (Beckman Instruments, Brea, CA) was used to determine culture OD$_{600}$, with vigorous shaking before each measurement. Bacterial enumeration was done by plate count from cultures prepared as described above and grown for 48 h.

Supernatant protein precipitation and protein quantification. Overnight aerated cultures were grown at 28°C in LB broth with or without appropriate antibiotics. Cells were diluted 1:100 into fresh LB broth with supplements, 11 mM glucose, 11 mM xylose, 11 mM sorbitol, 11 mM ribose, 22 mM or 44 mM glycerol, or 1 mM IPTG, as indicated. Cultures were incubated for 24 h at 28°C or 37°C. Cells were removed by centrifugation (4,000 × *g*/5 min/room temperature [RT]), supernatants passed through a 0.2-μm Acrodisc filter (Pall, Corp., Port Washington, NY), and mixed with ice-cold ethanol at a 1:4 ratio. Precipitation was allowed for 2 days at 4°C. Pellets were collected by centrifugation (8,000 × *g*/10 min/4°C) and air dried. Proteins were extracted with the urea buffer (24), resolved by SDS-PAGE (72), and stained with Coomassie blue. Supernatants from cultures grown with glycerol were subjected to protein quantification by Bradford assay (ThermoScientific, Waltham, MA) according to the manufacturer's protocol.

TEM. *Y. pestis* KIM6$^+$ Nal^r (KIM6$^+$ wild type) and the Δ*ail* mutant were incubated in LB broth with aeration at 37°C until mid-logarithmic phase (OD$_{600}$ of 0.8) or for 24 h. Cells were harvested at mid-logarithmic phase by centrifugation (2,000 × *g*/5 min/RT), washed in Tris-EDTA buffer, and fixed as previously described (11). Cells harvested at 24 h were mixed with the fixative at a 1:1 ratio without centrifugation. The following day, cells were postfixed with 2% OsO$_4$, stained with 1% tannic acid, and dehydrated (11), with the last dehydration step including acetone. Finally, samples were infiltrated with Spurr's and acetone, embedded in resin, polymerized, sectioned (some sections were stained with 4% uranyl acetate), and viewed with a Hitachi H600 or Philips transmission electron microscope.

Antibiotic and SDS sensitivity assays. Vancomycin (30 μg) discs from BD (Franklin Lakes, NJ) and vancomycin, novobiocin, and polymyxin B from Sigma (St. Louis, Mo) were used. Conventional Kirby-Bauer disc plate diffusion tests (73) were used to assess antibiotic sensitivity. Standard antibiotic MICs were determined using cultures in LB broth (74). Both tests were performed at 37°C. For the SDS sensitivity assay, overnight aerated cultures were grown at 28°C in LB broth. Cells were diluted 1:100 into fresh LB broth containing serially diluted SDS (0 to 780 μg/ml) and incubated for 24 h at 37°C. Absorbances at OD$_{600}$ were recorded and the half-maximal inhibitory concentration (IC$_{50}$) calculated. All assays were done in duplicate or triplicate on separate days.

MS to identify supernatant proteins. The Δ*ail* mutant was grown overnight at 28°C in LB broth with aeration. Cells were diluted 1:100 into fresh LB broth, incubated for 24 h at 37°C, and prepared as described for the supernatant protein precipitation as described above. Proteins were resolved by SDS-PAGE (72) and stained with Coomassie blue. A 2-mm-wide vertical strip spanning each lane of gel-resolved proteins was excised, divided into five parts, destained, and trypsinized (24, 75, 76). MS/MS

TABLE 3 Bacteria

Strain	Relevant genotype	Source or reference
Escherichia coli		
CC1118 λ*pir*	R$^-$ M$^+$ λ*pir*$^+$	80
S17-1 λ*pir*	Δ*recA* RP4 2-Tc::Mu-Kn::Tn7 λ*pir*$^+$ *tra*$^+$ Tp^r Str^r	80
TOP10	F$^-$ *mcrA* Δ(*mrr-hsdRMS-mcrBC*) φ80*lacZ*ΔM15 Δ*lacX74 nupG recA1 araD139* Δ(*ara-leu*)7697 *galE15 galK16 rpsL*(Str^r) *endA1*	Invitrogen
Yersinia pestis		
KIM6$^+$Nal^r	*pgm*$^+$ pCD1$^-$ pMT1$^+$ pPCP$^+$ Nal^r	24
KIM6$^+$Nal^r Δ*ail::npt* (previously Δ*ompX::npt*)	*pgm*$^+$ pCD1$^-$ pMT1$^+$ pPCP$^+$ Δ*ail* Nal^r Kn^r	24
KIM6$^+$Nal^r Δ*ail::npt/ail*$^+$ (previously Δ*ompX::npt/ompX*$^+$)	*pgm*$^+$ pCD1$^-$ pMT1$^+$ pPCP$^+$ *ail*$^+$ with integrated pMHZ2, Nal^r Kn^r Cm^r	24
KIM6$^+$Nal^r Δ*ail*	*pgm*$^+$ pCD1$^-$ pMT1$^+$ pPCP$^+$Δ*ail* Nal^r	This study
KIM5	*pgm* mutant pCD1$^+$ pMT1$^+$ pPCP$^+$	S. C. Straley, University of Kentucky
KIM5 Δ*ail::npt*	*pgm* mutant pCD1$^+$ pMT1$^+$ pPCP$^+$ Δ*ail* Kn^r	This study
KIM5 Δ*ail::npt/ail*$^+$	*pgm* mutant pCD1$^+$ pMT1$^+$ pPCP$^+$ *ail*$^+$ with integrated pMHZ2, Kn^r Cm^r	This study
KIM6$^+$ Nal^r Δ*ail*Δ*pst::npt*	*pgm*$^+$ pCD1$^-$ pMT1$^+$ pPCP$^+$ Δ*ail* Δ*pst* Nal^r Kn^r	This study
KIM6$^+$Nal^r Δ*ail pldA*::mini-Tn5	*pgm*$^+$ pCD1$^-$ pMT1$^+$ pPCP$^+$ Δ*ail pldA*::mini-Tn5*lacZ* Nal^r Kn^r	This study
KIM6$^+$Nal^r Δ*ail*Δ*pldA::npt*	*pgm*$^+$ pCD1 pMT1$^+$ pPCP$^+$ Δ*ail*Δ*pldA* Nal^r Kn^r	This study
KIM6$^+$Nal^r Δ*ail*Δ*pldA::npt/pldA*$^+$	*pgm*$^+$ pCD1$^-$ pMT1$^+$ pPCP$^+$Δ*ail pldA*$^+$ with integrated pMHZ5, Nal^r Kn^r Cm^r	This study
KIM6$^+$Nal^r Δ*pldA::npt*	*pgm*$^+$ pCD1$^-$ pMT1$^+$ pPCP$^+$ Δ*pldA* Nal^r Kn^r	This study
KIM6$^+$Nal^r Δ*pldA::npt/pldA*$^+$	*pgm*$^+$ pCD1$^-$ pMT1$^+$ pPCP$^+$ *pldA*$^+$ with integrated pMHZ5, Nal^r Kn^r Cm^r	This study
Enteropathogenic *Yersinia*		
Y. pseudotuberculosis	*ail*$^+$, patient isolate	P. Feng, FDA
Y. enterocolitica 8081c	O:8, *ail*$^+$, patient isolate	Laboratory collection

analysis using a Waters Nanoacquity ultraperformance liquid chromatography (UPLC) unit (Waters Corp., Milford, MA) was performed as described previously (24, 77). A ProteinLynx Global Server 2.2 and Protein Expression Informatics System software version 1.0 were used for MS/MS spectral analysis, peptide sequencing, and protein identification. MS/MS data were compared to the protein sequence databases of *Y. pestis* KIM from the University of Wisconsin (http://www.genome.wisc.edu/sequencing/pestis .htm) and *Y. pestis* CO92 from the Sanger Institute (http://www.sanger.ac.uk/Projects/Y_pestis/). Results were analyzed using Mascot software (Matrix Science, London, UK). Gene identities (ID) of protein products detected were recorded compared to the *Y. pestis* KIM genome.

Phage release assay. The Δ*ail* mutant was grown overnight at 28°C in LB broth with aeration. Cells were diluted 1:100 into fresh LB broth and incubated for 48 h at 37°C. A KIM6$^+$ wild-type culture was prepared as described above, except that at 40 h, 1.5 μg/ml mitomycin C (Sigma, St. Louis, Mo) was added. After incubation, bacteria were centrifuged (4,000 × *g*/5 min/4°C) and supernatants collected and passed through a 0.2-μm Acrodisc filter (Pall, Corp., Port Washington, NY). Bacteria to agar was prepared by mixing 10 μl of overnight cultures (grown in LB broth at 28°C with aeration) of KIM6$^+$ wild type, the Δ*ail* mutant, *Y. pseudotuberculosis*, or *Y. enterocolitica* 8081c, with 5 ml of tempered (45°C) 0.6% LB agar. Filtered supernatants (1, 10, or 100 μl) or medium controls with or without mitomycin C were added, mixed, and overlaid on LB agar (1.5%). Plates were incubated for 24 h at 28°C or 37°C.

Engineering of *ail* and *pst* deletion mutations. The *ail* deletion in *Y. pestis* KIM5 was made as previously described (24), except that single-crossover recombinants were counterselected on Cm CIN *Yersinia* agar plates. To make a double deletion Δ*ail* Δ*pst* mutant, the Kn^r (*npt*) cassette was removed using pPCP20 from *Y. pestis* KIM6$^+$ Δ*ail::npt* as described by Datsenko and Wanner (78). Deletion of pesticin (*pst*, *YPPCP1.05c*) utilized a combination of methods described by Smith (79) and Datsenko and Wanner (78). The Kn^r cassette flanked by the flippase recognition target (FRT) sites was amplified by PCR from pKD4 (78) and cloned in pEPSacB1 (79), generating the pEPSacB1Kan plasmid. Fragments homologous to 5′ and 3′ regions of *pst* were amplified by PCR and cloned on the opposite sites of the FRT-flanked Kn^r cassette. The resulting construct, pMHZ4, was transformed into *E. coli* S17-1 λ*pir* and a successful transformant was mated with the KIM6$^+$ wild type and Δ*ail* mutant. Single-crossover recombinants were counterselected on LB agar with Nal and Cm as described previously (24). The merodiploid strains (*pst*$^+$/*pst*::*npt*) served as an isogenic precursors for selecting the *pst*::*npt* disruptions. They were isolated on LB agar containing sucrose to select for a second crossover event while maintaining selection for the *pst::npt* disruption. Sucrose-resistant, Cm-sensitive colonies were tested by PCR and sequenced to confirm the deletion.

Caf1 capsule immunostaining. Immunostaining was done at RT; 2% bovine serum albumin in phosphate-buffered saline (PBS) was used as a blocking buffer and antibody diluent. Mouse anti-Caf1 antibody, clone YPF19 (Bio-Rad, Hercules, CA), was diluted at a ratio of 1:100, and goat anti-mouse Alexa

TABLE 4 Plasmids

Plasmid	Relevant genotype	Source or reference
pCP20	Temp-sensitive origin of replication and thermal induction of flippase synthesis; used to remove *npt* cassette from the deletion mutants, Amp^r Cm^r	78
pMHZ2	Δ*ail*::*npt* gene flanked by FRT sites, used for deletion of *ail*, Kn^r Cm^r	24
pEPSacB1	*mob*$^+$, *pir*-dependent *ori*R6K, *sacBR*$^+$ Cm^r	79
pEPSacB1Kan	*mob*$^+$, *pir*-dependent *ori*R6K, *sacBR*$^+$, with Kn^r cassette flanked with FRT sites, Kn^r Cm^r	This study
pTRC-Ail	Ail (*y1324*, OmpX) in pTrc99a, Amp^r	12
pTRC-*y1682*	*y1682* in pTrc99a, Amp^r	12
pTRC-*y2034*	*y2034* in pTrc99a, Amp^r	12
pTRC-*y2446*	*y2446* in pTrc99a, Amp^r	12
pMHZ4	pEP*sac*B1Kn containing Δ*pst*::*npt* used for deletion of pesticin, Kn^r Cm^r	This study
pUTmini-Tn*5lacZ*	Suicide plasmid for mini-Tn*5lacZ* delivery, Amp^r Kn^r	80
pBR322	Expression vector, Amp^r Tet^r	New England Biolabs, Inc.
pMHZ5	pEP*sac*B1Kn containing Δ*pldA*::*npt* used for deletion of phospholipase A, Kn^r Cm^r	This study
pUC19	Backbone vector used to clone *pldA*, Amp^r	New England Biolabs, Inc.
pPldA^{WT}	*y0396* and its 100-bp upstream regulatory fragment in pUC19, Amp^r	This study
pPldA^{S164A}	Catalytic mutant version of pPldA, Amp^r	This study
pBAD/HisA	Used as a template for cloning of the ampicillin resistance cassette, Amp^r	Invitrogen
pACYC177-*lux*	*luxCDABE* Kn^r	82
pACYC177-pmrl*slux*	Promoterless pACYC177-*lux*, contains SacI fragment with Amp^r cassette, Kn^r Amp^r	This study
pACYC177-*pldAlux*	*luxCDABE* under *Y. pestis pldA* promoter, Kn^r	This study
pACYC177-*pldAlux2*	*luxCDABE* under *Y. pestis pldA* promoter, contains SacI fragment with ampicillin resistance cassette, Kn^r Amp^r	This study
pACYC177-*rpoElux*	*luxCDABE* under *Y. pestis rpoE* promoter, Kn^r	This study
pACYC177-*rpoElux2*	*luxCDABE* under *Y. pestis rpoE* promoter, contains SacI fragment with ampicillin resistance cassette, Kn^r Amp^r	This study
pACYC177-*rpoHlux*	*luxCDABE* under *Y. pestis rpoH* promoter, Kn^r	This study
pACYC177-*rpoHlux2*	*luxCDABE* under *Y. pestis rpoH* promoter, contains SacI fragment with ampicillin resistance cassette, Kn^r Amp^r	This study
pDegP	*E. coli* DegP in pACYC184 under *trc* promoter, Cm^r	R. Misra, Arizona State University
pDegP^{S210A}	*E. coli* protease-deficient DegP in pACYC184 under *trc* promoter, Cm^r	R. Misra, Arizona State University
pBA169	pTrc99a ΔNcoI Amp^r	41
pRC136	*E. coli* H198P DegSΔPDZ-6His in pBA169, Amp^r	41

Fluor 546 antibody (ThermoFisher Scientific, Waltham, MA) antibody was diluted at a ratio of 1:500. KIM6$^+$ wild type and the Δ*ail* mutant were incubated in LB broth with or without 11 mM glucose at 37°C with aeration until mid-logarithmic phase (OD$_{600}$ of 0.8). Cultures (1 ml) were centrifuged (4,000 × g/5 min/RT) and resuspended in 50 μl PBS. Cells were spread on a glass slide, air dried, and heat fixed. Samples were blocked with blocking buffer for 1 h, washed once with blocking buffer, and incubated with primary anti-Caf1 antibody for 1 h. Samples were washed thrice for 5 min and stained with secondary anti-mouse Alexa Fluor 546 antibody. After 1 h, bacteria were washed thrice with PBS for 5 min. Samples were incubated 20 min with 300 nM DAPI (4′,6′-diamidino-2-phenylindole; ThermoFisher Scientific) in PBS to stain bacterial DNA, washed briefly 5 times, and mounted with ProLong Gold (ThermoFisher Scientific; Waltham, MA) antifade reagent. Cells were visualized with a Nikon Eclipse E1000 fluorescence microscope (Tokyo, Japan) with a 100× objective. Images were acquired using a Hamamatsu Orca digital camera (Hamamatsu, Japan) and Metamorph software (Molecular Devices, San Jose, CA).

Generalized transposon mutagenesis, library screening, and gene identification. *E. coli* S17-1 λ*pir* carrying p-mini-Tn*5lacZ* (80) and the Δ*ail* mutant were mated overnight on LB agar plate at RT in several independent experiments. After conjugation, cells were resuspended in 1 ml of LB broth and plated on LB agar supplemented with Kn and Nal to select for colonies with successful Tn*5* transpositions. After a 3-day incubation at 28°C, colonies were harvested and pooled into 500 ml LB broth with Nal, Kn, and 11 mM ribose to enrich for suppressors that did not lyse. Cultures were incubated 3 days with aeration at 37°C and diluted 1:100 into fresh LB broth with antibiotics and ribose, as described above. This cycle of selection was repeated twice. Lysis suppressors were verified by turbidity comparisons with the KIM6$^+$ wild type and the Δ*ail* mutant as positive and negative controls, respectively.

To identify lysis suppressor genes generated by Tn*5lacZ* insertions, total genomic DNA was purified, digested with EcoRI, cloned into the EcoRI-digested pBR322, transformed into *E. coli* TOP10, and selected for Kn^r. Plasmid DNA was purified and sequenced across the transposon junction using the primer positioned upstream from the transposon 3′ end, and *Y. pestis* flanking DNA was identified by a standard BLAST search of the *Y. pestis* KIM genome.

Genetic manipulations of *pldA*. Deletion of *pldA* (*y0396*) was performed as described above for the *pst* deletion, with the pMHZ5 construct used for mating and Cm CIN *Yersinia* agar used for selection of the first crossover mutant. For *pldA* expression in *trans*, the *pldA* structural gene (*y0396*) and its regulatory region (100-bp upstream region) was cloned into BamHI- and HindIII-digested pUC19 vector. The

TABLE 5 Primers

Application and characteristics	Primer sequence(s)[a]
Primers for the pMHZ2 Kn[r] cassette with NotI and SmaI restriction sites	5'ATATATAGCGGCCGCAGATTGCAGCATTAC3' (F), 5'ATATACCCGGGCACAGGAACACTTAACG3' (R)
Primers for *pst* 5'-deletion mutation with SacI and NotI restriction sites	5'TATAGAGCTCTCTTTTTGCACCAGAGCGC3' (F), 5'TATAAGCGGCCGCAAAAAGGGTTTAAGTTAT5' (R)
Primers for *pst* 3'-deletion mutation with SmaI/XmaI and EcoRV restriction sites	5'ATATACCCGGGAGTTTAAAATTACTCCGGCC3' (F), 5'GCGGAGGATATCATGTCAGATACAATGGTA3' (R)
Sequencing primer for identification of the Tn5*lacZ* insertion junctions	5'TTACGCTGACTTGACGGGAC3' (F)
Primers for *pldA* 5'-deletion mutation with SacI and NotI restriction sites	5'ATATAGAGCTCATGGCGAGATTTTGGCAGA3' (F), 5'ATATAGCGGCCGCATAAAGTAGGAAAGGATTA3' (R)
Primers for *pldA* 3'-deletion mutation with SmaI/XmaI and EcoRV restriction sites	5'TATTACCCGGGATGGTCGCTATAACTGGAA3' (F), 5'ATGCGCGATATCTTAAAGGACATCGTTCAACAT3' (R)
Primers for *pldA* and its 100-bp upstream regulatory fragment with BamHI and HindIII restriction sites	5' TATATGGATCCAAATCATAAAGATAAACAACA3' (F), 5'TATAT AAGCTTTTAAAGGACATCGTTCAACAT3' (R)
PldA[S164A] mutagenesis primers	5'TAACCATCAAGCCAACGGTAAA G3' (F), 5'AAACCAAATTCGACTTCGC3' (R)
Sequencing primers to confirm PldA[S164A] point mutation	5'GGCGATTAAGTTGGGTAACGC3' (F), 5'ATGGCACCCCAGGCTTTACAC3' (R)
Primers for 221-bp *pldA* promoter with BamHI restriction sites	5'GCGCGCGGATCCTATGTTCTATTCTCTTC3' (F), 5'ATATATGGATCCAATTCCCTCACCACCCTC3' (R)
Primers for 187-bp *rpoE* promoter with BamHI restriction sites	5'GTATAGGATCCGTTAGCCTATCTGCTCAAG3' (F), 5'ATATAGGATCCCCGAGGTGAACTCTCCC3' (R)
Primers for 300-bp *rpoH* promoter with BamHI restriction sites	5'ATATGGGATCCTTATACTCTTTCCTTACC3' (F), 5'TATATGGATCCTTAAACCCTCTCAGT3' (R)
Sequencing primer for *rpoE*, *rpoH*, and *pldA* promoter orientation in pACYAC117-prls*lux*	5'GGCAGACCTCAGCGCTCAAAGA3' (F),
Primers for the Amp[r] cassette from pBAD/HisA with SacI restriction sites	5'GCGCGGAGCTCTTTTGTTTATTTTTCTAAAT3' (F), 5'ATATAGAGCTCAAACTTGGTCTGACAGTTAC3' (R)

[a]F, forward; R, reverse.

point mutation (PldA[S164A]), disrupting PldA enzymatic activity, was generated using a Q5 site-directed mutagenesis kit (New England Biolabs, Inc.; Ipswich, MA). This site-directed mutagenesis was based on the findings of PldA catalytic activity in *E. coli* (81) and sequence homology with *Y. pestis pldA*.

Gene reporter systems utilizing the *lux* operon. To measure gene expression of *pldA*, *rpoE*, *rpoH*, and *lux* operon fusions were constructed. The KIM6^{+} wild-type *pldA*, *rpoE*, and *rpoH* promoters, on BamHI fragments (187 bp, 221 bp, and 300 bp, respectively), were cloned in front of the *lux* operon from *Vibrio harveyi* to generate reporters pACYC177- *pldAlux*, pACYC177-*rpoElux*, and pACYC177-*rpoHlux*. The correct orientation of the inserts was verified using the primers (Table 4). The SacI fragment containing the Amp[r] cassette from pBAD/HisA (Invitrogen, Waltham, MA) was inserted into the plasmids (described above), creating pACYC177-*pldAlux*2, pACYC177-*rpoElux*2, and pACYC177-*rpoHlux*2. *Y. pestis* strains were transformed with these plasmids and compared to controls transformed with the promoter-less pACYC177-pmrls*lux* to measure background luminescence. Overnight cultures grown in LB Amp broth at 28°C with aeration were diluted (1:5,000) in fresh LB Amp broth with or without supplements and incubated at 28°C or 37°C to an OD_{600} of 1 or 0.8 for cultures supplemented with glucose. Luminescence was measured in white 96-well plates using the SpectraMax L (Molecular Devices, LLC, San Diego, CA) and an endpoint measurement with 1-s integration time. Data are presented as luminescence units/OD_{600} after adjustment for background luminescence.

DegP expression. KIM6^{+} wild-type, Δ*ail*, Δ*ail* pDegP, and Δ*ail* pDegP[S210A] strains were grown overnight in LB broth with or without Cm at 28°C with aeration. Cells were diluted 1:100 in fresh LB broth with or without 1 mM IPTG and Cm and incubated at 37°C for 48 h, and cell densities (OD_{600}) were compared.

***rpoE* induction.** To measure induction of *rpoE* by H198PDegSΔPDZ, overnight cultures of KIM6^{+} wild-type pACYC177-*rpoElux*, Δ*ail* pACYC177-*rpoElux*, Δ*ail* pBA16 pACYC177-*rpoElux*, and Δ*ail* pRC136 pACYC177-*rpoElux* were prepared with appropriate antibiotics as described above. Cultures were diluted (1:5,000) in LB broth with 1 mM IPTG and appropriate antibiotics and incubated at 37°C to an OD_{600} of 1, and luminescence measured as described above.

To test the role of PldA in H198PDegSΔPDZ-dependent lysis, overnight cultures of KIM6^{+} wild-type, Δ*ail*, Δ*pldA*, Δ*ail* Δ*pldA*, KIM6^{+} wild-type pBA169, Δ*ail* pBA169, Δ*pldA* pBA169, Δ*ail* Δ*pldA* pBA169, KIM6^{+} wild-type pRC136, Δ*ail* pRC136, Δ*pldA* pRC136, and Δ*ail* Δ*pldA* pRC136 strains were prepared as described above. Cell lysis was determined by spotting serial dilutions on LB agar plates containing 1 mM IPTG with or without appropriate antibiotics. Plates were observed for colony clearing after incubation at 28°C or 37°C for 8 days. To determine if *pldA* was part of the RpoE regulon, cultures of the Δ*ail* mutant, Δ*ail* pBA169, and Δ*ail* pRC136, each transformed with pACYC177-*pldAlux*, were grown as described above for the gene reporter systems utilizing the *lux* operon, except that H198PDegSΔPDZ was induced with 1 mM IPTG.

Statistical analysis. Data were analyzed using the Student's *t* test with one-way or two-way analysis of variance (ANOVA). Effects of temperature, glucose, and Ca^{2+} on *pldA* expression was tested with the

two-way ANOVA without interactions; growth at 28°C versus 37°C, growth in LB versus LB supplemented with glucose, and growth in LB versus LB supplemented with Ca^{2+} were analyzed. The absolute IC_{50} was calculated using four-parameter logistic nonlinear regression. These analyses were conducted with SigmaPlot or R software.

SUPPLEMENTAL MATERIAL

Supplemental material is available online only.

SUPPLEMENTAL FILE 1, PDF file, 0.9 MB.

ACKNOWLEDGMENTS

REFERENCES

1. Silhavy TJ, Kahne D, Walker S. 2010. The bacterial cell envelope. Cold Spring Harb Perspect Biol 2:a000414. https://doi.org/10.1101/cshperspect.a000414.

2. Nikaido H, Vaara M. 1985. Molecular basis of bacterial outer membrane permeability. Microbiol Rev 49:1–32. https://doi.org/10.1128/mr.49.1.1-32.1985.

3. Malinverni JC, Silhavy TJ. 2009. An ABC transport system that maintains lipid asymmetry in the Gram-negative outer membrane. Proc Natl Acad Sci U S A 106:8009–8014. https://doi.org/10.1073/pnas.0903229106.

4. Sutterlin HA, Shi H, May KL, Miguel A, Khare S, Huang KC, Silhavy TJ. 2016. Disruption of lipid homeostasis in the Gram-negative cell envelope activates a novel cell death pathway. Proc Natl Acad Sci U S A 113:1565–1574. https://doi.org/10.1073/pnas.1601375113.

5. Nikaido H. 2005. Restoring permeability barrier function to outer membrane. Chem Biol 12:507–509. https://doi.org/10.1016/j.chembiol.2005.05.001.

6. Dekker N. 2000. Outer-membrane phospholipase A: known structure, unknown biological function. Mol Microbiol 35:711–717. https://doi.org/10.1046/j.1365-2958.2000.01775.x.

7. Kamischke C, Fan J, Bergeron J, Kulasekara HD, Dalebroux ZD, Burrell A, Kollman JM, Miller SI. 2019. The *Acinetobacter baumannii* Mla system and glycerophospholipid transport to the outer membrane. ELife 8:40171. https://doi.org/10.7554/eLife.40171.

8. Powers MJ, Trent MS. 2019. Intermembrane transport: glycerophospholipid homeostasis of the Gram-negative cell envelope. Proc Natl Acad Sci U S A 116:17147–17155. https://doi.org/10.1073/pnas.1902026116.

9. Powers MJ, Trent MS. 2018. Phospholipid retention in the absence of asymmetry strengthens the outer membrane permeability barrier to last-resort antibiotics. Proc Natl Acad Sci U S A 115:E8518–E8527. https://doi.org/10.1073/pnas.1806714115.

10. Prior JL, Parkhill J, Hitchen PG, Mungall KL, Stevens K, Morris HR, Reason AJ, Oyston PC, Dell A, Wren BW, Titball RW. 2001. The failure of different strains of *Yersinia pestis* to produce lipopolysaccharide O-antigen under different growth conditions is due to mutations in the O-antigen gene cluster. FEMS Microbiol Lett 197:229–233. https://doi.org/10.1111/j.1574-6968.2001.tb10608.x.

11. Kolodziejek AM, Schnider DR, Rohde HN, Wojtowicz AJ, Bohach GA, Minnich SA, Hovde CJ. 2010. Outer membrane protein X (Ail) contributes to *Yersinia pestis* virulence in pneumonic plague and its activity is dependent on the lipopolysaccharide core length. Infect Immun 78:5233–5243. https://doi.org/10.1128/IAI.00783-10.

12. Bartra SS, Styer KL, O'Bryant DM, Nilles ML, Hinnebusch BJ, Aballay A, Plano GV. 2008. Resistance of *Yersinia pestis* to complement-dependent killing is mediated by the Ail outer membrane protein. Infect Immun 76:612–622. https://doi.org/10.1128/IAI.01125-07.

13. Chandler CE, Harberts EM, Pelletier MR, Thaipisuttikul I, Jones JW, Hajjar AM, Sahl JW, Goodlett DR, Pride AC, Rasko DA, Trent MS, Bishop RE, Ernst RK. 2020. Early evolutionary loss of the lipid A modifying enzyme PagP resulting in innate immunity evasion in *Yersinia pestis*. Proc Natl Acad Sci U S A 117:22984–22991. https://doi.org/10.1073/pnas.1917504117.

14. Montminy SW, Khan N, McGrath S, Walkowicz MJ, Sharp F, Conlon JE, Fukase K, Kusumoto S, Sweet C, Miyake K, Akira S, Cotter RJ, Goguen JD, Lien E. 2006. Virulence factors of *Yersinia pestis* are overcome by a strong lipopolysaccharide response. Nat Immunol 7:1066–1073. https://doi.org/10.1038/ni1386.

15. Barondess JJ, Beckwith J. 1990. A bacterial virulence determinant encoded by lysogenic coliphage lambda. Nature 346:871–874. https://doi.org/10.1038/346871a0.

16. Mecsas J, Rouviere PE, Erickson JW, Donohue TJ, Gross CA. 1993. The activity of sigma E, an *Escherichia coli* heat-inducible sigma-factor, is modulated by expression of outer membrane proteins. Genes Dev 7:2618–2628. https://doi.org/10.1101/gad.7.12b.2618.

17. Climent N, Ferrer S, Rubires X, Merino S, Tomas JM, Regue M. 1997. Molecular characterization of a 17-kDa outer-membrane protein from *Klebsiella pneumoniae*. Res Microbiol 148:133–143. https://doi.org/10.1016/S0923-2508(97)87644-9.

18. Kim K, Kim KP, Choi J, Lim JA, Lee J, Hwang S, Ryu S. 2010. Outer membrane proteins A (OmpA) and X (OmpX) are essential for basolateral invasion of *Cronobacter sakazakii*. Appl Environ Microbiol 76:5188–5198. https://doi.org/10.1128/AEM.02498-09.

19. Stoorvogel J, van Bussel MJ, Tommassen J, van de Klundert JA. 1991. Molecular characterization of an *Enterobacter cloacae* outer membrane protein (OmpX). J Bacteriol 173:156–160. https://doi.org/10.1128/jb.173.1.156-160.1991.

20. Heffernan EJ, Harwood J, Fierer J, Guiney D. 1992. The *Salmonella typhimurium* virulence plasmid complement resistance gene *rck* is homologous to a family of virulence-related outer membrane protein genes, including *pagC* and *ail*. J Bacteriol 174:84–91. https://doi.org/10.1128/jb.174.1.84-91.1992.

21. Bliska JB, Falkow S. 1992. Bacterial resistance to complement killing mediated by the Ail protein of *Yersinia enterocolitica*. Proc Natl Acad Sci U S A 89:3561–3565. https://doi.org/10.1073/pnas.89.8.3561.

22. Yang Y, Merriam JJ, Mueller JP, Isberg RR. 1996. The *psa* locus is responsible for thermoinducible binding of *Yersinia pseudotuberculosis* to cultured cells. Infect Immun 64:2483–2489. https://doi.org/10.1128/iai.64.7.2483-2489.1996.

23. Kolodziejek AM, Hovde CJ, Minnich SA. 2012. *Yersinia pestis* Ail: multiple roles of a single protein. Front Cell Infect Microbiol 2:103. https://doi.org/10.3389/fcimb.2012.00103.

24. Kolodziejek AM, Sinclair DJ, Seo KS, Schnider DR, Deobald CF, Rohde HN, Viall AK, Minnich SS, Hovde CJ, Bohach GA. 2007. Phenotypic characterization of OmpX, an Ail homologue of *Yersinia pestis* KIM. Microbiology 153:2941–2951. https://doi.org/10.1099/mic.0.2006/005694-0.

25. Singh C, Lee H, Tian Y, Bartra SS, Hower S, M FL, Yao Y, Ivanov AY, Shaikhutdinova RZ, Anisimov AP, Plano GV, Im W, Marassi FM. 2020. Mutually constructive roles of Ail and LPS in *Yersinia pestis* serum survival. Mol Microbiol 114:510–520. https://doi.org/10.1111/mmi.14530.

26. Felek S, Krukonis ES. 2009. The *Yersinia pestis* Ail protein mediates binding and Yop delivery to host cells required for plague virulence. Infect Immun 77:825–836. https://doi.org/10.1128/IAI.00913-08.

27. Tsang TM, Felek S, Krukonis ES. 2010. Ail binding to fibronectin facilitates *Yersinia pestis* binding to host cells and Yop delivery. Infect Immun 78: 3358–3368. https://doi.org/10.1128/IAI.00238-10.

28. Hinnebusch BJ, Jarrett CO, Callison JA, Gardner D, Buchanan SK, Plano GV. 2011. Role of the *Yersinia pestis* Ail protein in preventing a protective polymorphonuclear leukocyte response during bubonic plague. Infect Immun 79:4984–4989. https://doi.org/10.1128/IAI.05307-11.

29. Pierson DE, Falkow S. 1993. The *ail* gene of *Yersinia enterocolitica* has a role in the ability of the organism to survive serum killing. Infect Immun 61:1846–1852. https://doi.org/10.1128/iai.61.5.1846-1852.1993.

30. Myers-Morales T, Cowan C, Gray ME, Wulff CR, Parker CE, Borchers CH, Straley SC. 2007. A surface-focused biotinylation procedure identifies the *Yersinia pestis* catalase KatY as a membrane-associated but non-surface-located protein. Appl Environ Microbiol 73:5750–5759. https://doi.org/10.1128/AEM.02968-06.

31. Perry RD, Bobrov AG, Kirillina O, Jones HA, Pedersen L, Abney J, Fetherston JD. 2004. Temperature regulation of the hemin storage (Hms+) phenotype of *Yersinia pestis* is posttranscriptional. J Bacteriol 186:1638–1647. https://doi.org/10.1128/JB.186.6.1638-1647.2004.

32. Demeure CE, Dussurget O, Fiol GM, Le Guern A, Savin C, Pizarro-Cerda J. 2019. *Yersinia pestis* and plague: an updated view on evolution, virulence determinants, immune subversion, vaccination, and diagnostics. Genes Immun 20:357–370. https://doi.org/10.1038/s41435-019-0065-0.

33. Sebbane F, Jarrett C, Gardner D, Long D, Hinnebusch BJ. 2009. The *Yersinia pestis caf*1M1A1 fimbrial capsule operon promotes transmission by flea bite in a mouse model of bubonic plague. Infect Immun 77:1222–1229. https://doi.org/10.1128/IAI.00950-08.

34. Du Y, Rosqvist R, Forsberg A. 2002. Role of fraction 1 antigen of *Yersinia pestis* in inhibition of phagocytosis. Infect Immun 70:1453–1460. https://doi.org/10.1128/IAI.70.3.1453-1460.2002.

35. Janssen WA, Surgalla MJ. 1969. Plague bacillus: survival within host phagocytes. Science 163:950–952. https://doi.org/10.1126/science.163.3870.950.

36. Sebbane F, Jarrett CO, Gardner D, Long D, Hinnebusch BJ. 2006. Role of the *Yersinia pestis* plasminogen activator in the incidence of distinct septicemic and bubonic forms of flea-borne plague. Proc Natl Acad Sci U S A 103:5526–5530. https://doi.org/10.1073/pnas.0509544103.

37. Lim B, Miyazaki R, Neher S, Siegele DA, Ito K, Walter P, Akiyama Y, Yura T, Gross CA. 2013. Heat shock transcription factor σ^{32} co-opts the signal recognition particle to regulate protein homeostasis in *Escherichia coli*. PLoS Biol 11:e1001735. https://doi.org/10.1371/journal.pbio.1001735.

38. Nonaka G, Blankschien M, Herman C, Gross CA, Rhodius VA. 2006. Regulon and promoter analysis of the *E. coli* heat-schock factor, σ^{32}, reveals a mulitfaceted cellular response to heat stress. Genes Dev 20:1776–1789. https://doi.org/10.1101/gad.1428206.

39. Klein G, Raina S. 2015. Regulated control of the assembly and diversity of LPS by noncoding sRNAs. BioMed Res Int 2015:153561. https://doi.org/10.1155/2015/153561.

40. Roncarati D, Scarlato V. 2017. Regulation of heat-shock genes in bacteria: from signal sensing to gene expression output. FEMS Microbiol Rev 41: 549–574. https://doi.org/10.1093/femsre/fux015.

41. Chaba R, Alba BM, Guo MS, Sohn J, Ahuja N, Sauer RT, Gross CA. 2011. Signal integration by DegS and RseB governs the σE-mediated envelope stress response in *Escherichia coli*. Proc Natl Acad Sci U S A 108:2106–2111. https://doi.org/10.1073/pnas.1019277108.

42. De Las Penas A, Connolly L, Gross CA. 1997. SigmaE is an essential sigma factor in *Escherichia coli*. J Bacteriol 179:6862–6864. https://doi.org/10.1128/jb.179.21.6862-6864.1997.

43. Catalao MJ, Gil F, Moniz-Pereira J, Sao-Jose C, Pimentel M. 2013. Diversity in bacterial lysis systems: bacteriophages show the way. FEMS Microbiol Rev 37:554–571. https://doi.org/10.1111/1574-6976.12006.

44. Vollmer W, Pilsl H, Hantke K, Holtje JV, Braun V. 1997. Pesticin displays muramidase activity. J Bacteriol 179:1580–1583. https://doi.org/10.1128/jb.179.5.1580-1583.1997.

45. Braun V, Schaller K, Wabl RM. 1974. Isolation, characterization, and action of colicin M. Antimicrob Agents Chemother 5:520–533. https://doi.org/10.1128/AAC.5.5.520.

46. Guisbert E, Rhodius VA, Ahuja N, Witkin E, Gross CA. 2007. Hfq modulates the σ^{E}-mediated envelope stress response and the σ^{32}-mediated cytoplasmic stress response in *Escherichia coli*. J Bacteriol 189:1963–1973. https://doi.org/10.1128/JB.01243-06.

47. Skórko-Glonek J, Wawrzynów A, Krzewski K, Kurpierz K, Lipińska B. 1995. Site-directed mutagenesis of the HtrA (DegP) serine protease, whose proteolytic activity is indispensable for *Escherichia coli* survival at elevated temperatures. Gene 163:47–52. https://doi.org/10.1016/0378-1119(95)00406-v.

48. Yeow J, Tan KW, Holdbrook DA, Chong ZS, Marzinek JK, Bond PJ, Chng SS. 2018. The architecture of the OmpC-MlaA complex sheds light on the maintenance of outer membrane lipid asymmetry in *Escherichia coli*. J Biol Chem 293:11325–11340. https://doi.org/10.1074/jbc.RA118.002441.

49. Chong ZS, Woo WF, Chng SS. 2015. Osmoporin OmpC forms a complex with MlaA to maintain outer membrane lipid asymmetry in *Escherichia coli*. Mol Microbiol 98:1133–1146. https://doi.org/10.1111/mmi.13202.

50. Ruiz N, Kahne D, Silhavy TJ. 2006. Advances in understanding bacterial outer-membrane biogenesis. Nat Rev Microbiol 4:57–66. https://doi.org/10.1038/nrmicro1322.

51. Chatterjee A, Chaudhuri S, Saha G, Gupta S, Chowdhury R. 2004. Effect of bile on the cell surface permeability barrier and efflux system of *Vibrio cholerae*. J Bacteriol 186:6809–6814. https://doi.org/10.1128/JB.186.20.6809-6814.2004.

52. Shafer WM, Casey SG, Spitznagel JK. 1984. Lipid A and resistance of *Salmonella typhimurium* to antimicrobial granule proteins of human neutrophil granulocytes. Infect Immun 43:834–838. https://doi.org/10.1128/iai.43.3.834-838.1984.

53. Pieper R, Huang ST, Robinson JM, Clark DJ, Alami H, Parmar PP, Perry RD, Fleischmann RD, Peterson SN. 2009. Temperature and growth phase influence the outer-membrane proteome and the expression of a type VI secretion system in *Yersinia pestis*. Microbiology 155:498–512. https://doi.org/10.1099/mic.0.022160-0.

54. Motin VL, Georgescu AM, Fitch JP, Gu PP, Nelson DO, Mabery SL, Garnham JB, Sokhansanj BA, Ott LL, Coleman MA, Elliott JM, Kegelmeyer LM, Wyrobek AJ, Slezak TR, Brubaker RR, Garcia E. 2004. Temporal global changes in gene expression during temperature transition in *Yersinia pestis*. J Bacteriol 186: 6298–6305. https://doi.org/10.1128/JB.186.18.6298-6305.2004.

55. Lusk JE, Williams RJ, Kennedy EP. 1968. Magnesium and the growth of *Escherichia coli*. J Biol Chem 243:2618–2624. https://doi.org/10.1016/S0021-9258(18)93417-4.

56. Clifton LA, Skoda MWA, Le Brun AP, Ciesielski F, Kuzmenko I, Holt SH, Lakey JH. 2015. Effect of divalent cation removal on the structure of gram-negative bacterial outer membrane models. Langmuir 31:404–412. https://doi.org/10.1021/la504407v.

57. Becerra-Tomas N, Estruch R, Bullo M, Casas R, Diaz-Lopez A, Basora J, Fito M, Serra-Majem L, Salas-Salvado J. 2014. Increased serum calcium levels and risk of type 2 diabetes in individuals at high cardiovascular risk. Diabetes Care 37:3084–3091. https://doi.org/10.2337/dc14-0898.

58. Bishop RE. 2008. Structural biology of membrane-intrinsic beta-barrel enzymes: sentinels of the bacterial outer membrane. Biochim Biophys Acta 1778:1881–1896. https://doi.org/10.1016/j.bbamem.2007.07.021.

59. Bishop RE. 2005. The lipid A palmitoyltransferase PagP: molecular mechanisms and role in bacterial pathogenesis. Mol Microbiol 57:900–912. https://doi.org/10.1111/j.1365-2958.2005.04711.x.

60. Groisman EA. 2001. The pleiotropic two-component regulatory system PhoP-PhoQ. J Bacteriol 183:1835–1842. https://doi.org/10.1128/JB.183.6.1835-1842.2001.

61. Karow M, Fayet O, Cegielska A, Ziegelhoffer T, Georgopoulos C. 1991. Isolation and characterization of the *Escherichia coli htrB* gene, whose product is essential for bacterial viability above 33 degrees C in rich media. J Bacteriol 173:741–750. https://doi.org/10.1128/jb.173.2.741-750.1991.

62. Gronow S, Brade H. 2000. Lipopolysaccharide biosynthesis: which steps do bacteria need to survive? J Endotoxin Res 7:3–23.

63. Hayden JD, Ades SE. 2008. The extracytoplasmic stress factor, sigmaE, is required to maintain cell envelope integrity in *Escherichia coli*. PLoS One 3:e1573. https://doi.org/10.1371/journal.pone.0001573.

64. Rhodius VA, Suh WC, Nonaka G, West J, Gross CA. 2006. Conserved and variable functions of the sigmaE stress response in related genomes. PLoS Biol 4:e2. https://doi.org/10.1371/journal.pbio.0040002.

65. Valentin-Hansen P, Johansen J, Rasmussen AA. 2007. Small RNAs controlling outer membrane porins. Curr Opin Microbiol 10:152–155. https://doi.org/10.1016/j.mib.2007.03.001.

66. Murata M, Noor R, Nagamitsu H, Tanaka S, Yamada M. 2012. Novel pathway directed by sigma E to cause cell lysis in *Escherichia coli*. Genes Cells 17:234–247. https://doi.org/10.1111/j.1365-2443.2012.01585.x.

67. Kabir MS, Yamashita D, Koyama S, Oshima T, Kurokawa K, Maeda M, Tsunedomi R, Murata M, Wada C, Mori H, Yamada M. 2005. Cell lysis directed by sigmaE in early stationary phase and effect of induction of the *rpoE* gene on global gene expression in *Escherichia coli*. Microbiology 151:2721–2735. https://doi.org/10.1099/mic.0.28004-0.

68. Nicoloff H, Gopalkrishnan S, Ades SE. 2017. Appropriate regulation of the sigmaE-dependent envelope stress response is necessary to maintain cell envelope integrity and stationary-phase survival in *Escherichia coli*. J Bacteriol 199:e00089-17. https://doi.org/10.1128/JB.00089-17.

69. Dutta SK, Yao Y, Marassi FM. 2017. Structural insights into the *Yersinia pestis* outer membrane protein Ail in lipid bilayers. J Phys Chem B 121:7561–7570. https://doi.org/10.1021/acs.jpcb.7b03941.

70. Bertani G. 2004. Lysogeny at mid-twentieth century: P1, P2, and other experimental systems. J Bacteriol 186:595–600. https://doi.org/10.1128/JB.186.3.595-600.2004.

71. Surgalla MJ, Beesley ED. 1969. Congo red-agar plating medium for detecting pigmentation in *Pasteurella pestis*. Appl Microbiol 18:834–837. https://doi.org/10.1128/am.18.5.834-837.1969.

72. Laemmli UK. 1970. Cleavage of structural proteins during the assembly of the head of bacteriophage T4. Nature 227:680–685. https://doi.org/10.1038/227680a0.

73. Shaffer J, Goldin M (ed). 1974. Clinical diagnosis by laboratory methods. W.B. Saunders Company, Philadelphia, PA.

74. Andrews JM. 2001. Determination of minimum inhibitory concentrations. J Antimicrob Chemother 48:5–16. https://doi.org/10.1093/jac/48.suppl_1.5.

75. Shevchenko A, Wilm M, Vorm O, Mann M. 1996. Mass spectrometric sequencing of proteins silver-stained polyacrylamide gels. Anal Chem 68:850–858. https://doi.org/10.1021/ac950914h.

76. Katayama H, Nagasu T, Oda Y. 2001. Improvement of in-gel digestion protocol for peptide mass fingerprinting by matrix-assisted laser desorption/ionization time-of-flight mass spectrometry. Rapid Commun Mass Spectrom 15:1416–1421. https://doi.org/10.1002/rcm.379.

77. Hermans PW, Adrian PV, Albert C, Estevao S, Hoogenboezem T, Luijendijk IH, Kamphausen T, Hammerschmidt S. 2006. The streptococcal lipoprotein rotamase A (SlrA) is a functional peptidyl-prolyl isomerase involved in pneumococcal colonization. J Biol Chem 281:968–976. https://doi.org/10.1074/jbc.M510014200.

78. Datsenko KA, Wanner BL. 2000. One-step inactivation of chromosomal genes in *Escherichia coli* K-12 using PCR products. Proc Natl Acad Sci U S A 97:6640–6645. https://doi.org/10.1073/pnas.120163297.

79. Smith MJ. 2000. Genetic regulation of type III secretion systems in Yersinia enterocolitica. University of Idaho, Moscow, ID.

80. de Lorenzo V, Herrero M, Jakubzik U, Timmis KN. 1990. Mini-Tn*5* transposon derivatives for insertion mutagenesis, promoter probing, and chromosomal insertion of cloned DNA in gram-negative eubacteria. J Bacteriol 172:6568–6572. https://doi.org/10.1128/jb.172.11.6568-6572.1990.

81. Brok RG, Belandia IU, Dekker N, Tommassen J, Verheij HM. 1996. *Escherichia coli* outer membrane phospholipase A: role of two serines in enzymatic activity. Biochemistry 35:7787–7793. https://doi.org/10.1021/bi952970i.

82. Seo KS, Kim JW, Park JY, Viall AK, Minnich SS, Rohde HN, Schnider DR, Lim SY, Hong JB, Hinnebusch BJ, O'Loughlin JL, Deobald CF, Bohach GA, Hovde CJ, Minnich SA. 2012. The role of an intimin/invasin/autotransporter-like protein (Ilp) in *Yersinia pestis* virulence. Infect Immun 80:3559–3569. https://doi.org/10.1128/IAI.00294-12.